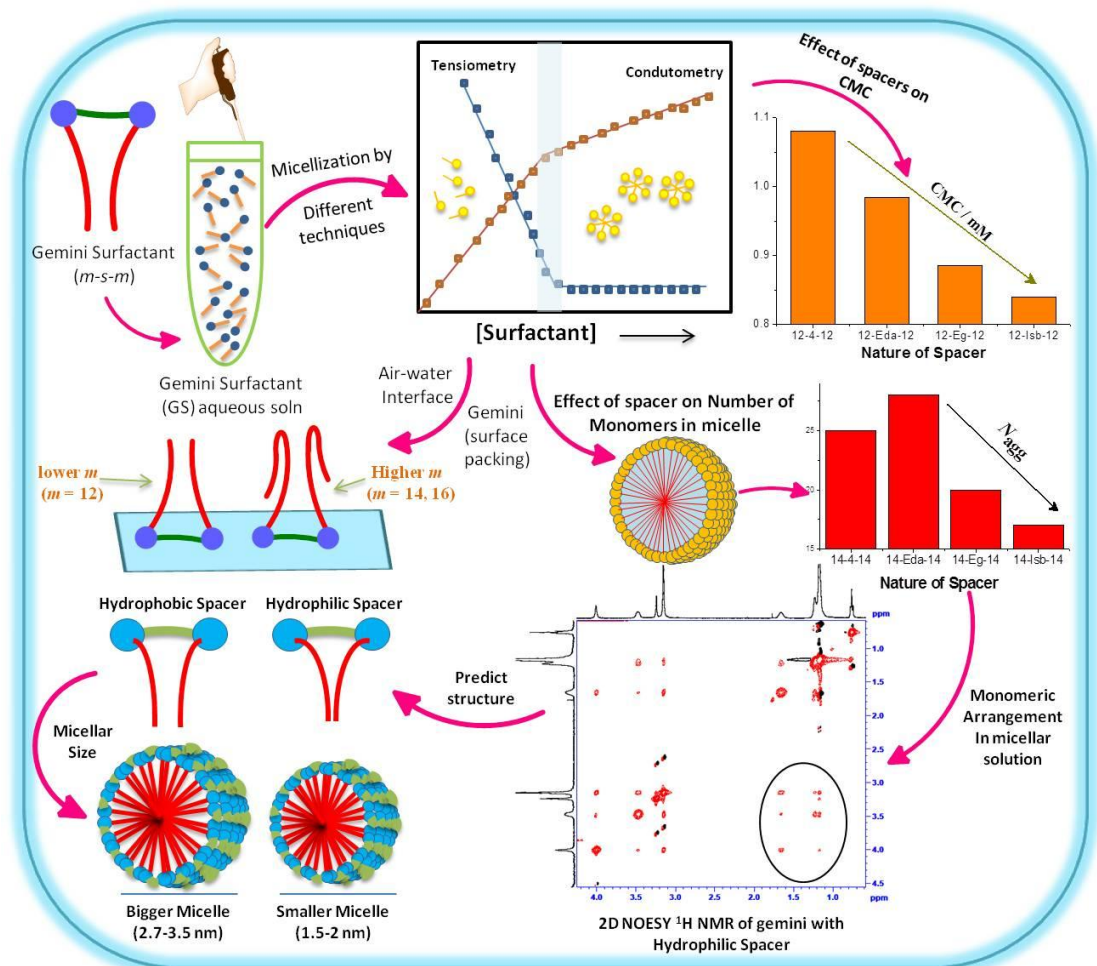


# Chapter 3

## Physico-chemical Behavior of Aqueous Gemini Surfactant Solution



### 3.1. Introduction

During the past few decades, association structures produced by a self-assembly processing have received considerable attention due to their dynamic nature [1]. The molecular self-assembly (*e.g.*, micelle) of the surfactants is ideally suitable for the construction of the responsive material since the dynamic and reversible conformational changes can be triggered by external stimuli (solvent, temperature, pH, *etc.*). Inclusion of different types of additives (salts, alcohols, sugars, ureas, hydrocarbons, *etc.*) is well-known to influence the micellar properties (*e.g.*, cmc) by affecting the solvent structure or morphology [2-6]. cmc is the first and foremost property to be known for all the newly synthesized surfactants before their use for any kind of application. Surfactant solutions have a general tendency to solubilize a certain amount of additive depending upon its polarity [7].

It is well documented that the cmc of surfactant varies with temperature [8]. The variation of cmc with temperature observed for ionic surfactants is different than their non-ionic counterparts. Generally, cmc of non-ionic surfactants decreases regularly with increase in temperature (till cloud point). However, ionic surfactants show a more interesting behavior: cmc decreases to a certain value ( $cmc_m$ ) and then increases with continuous increase in temperature (U-shaped behavior) [8-12]. The temperature at  $cmc_m$  ( $T_m$ ) for both non-ionic and ionic surfactants increases as the hydrophobicity of the surfactant decreases. The temperature effect on the cmc can also be used to obtain various thermodynamic parameters of micellization. Further, the micellization process has been reported to exhibit an enthalpy – entropy compensation [13].

Recently, the temperature effect on micellization of gemini surfactants has also been studied [2, 5, 14-26]. However, only a few studies reported a minimum in the cmc vs temperature plot [17, 26]. Similarly, no serious attempt has been made to study enthalpy – entropy compensation in gemini surfactant micellization process. Spacer has remarkable effect on the micellization properties of the gemini surfactant (please see Chapter 1). For hydrophilic spacer, the cmc increases with progressive increase in spacer chain length [27]. However, the cmc passes through a broad maximum with increasing the spacer length of a hydrophobic spacer [28].

In this Chapter, micellization behavior for all the synthesized gemini surfactants (included in Chapter 2) in aqueous solution (or aqueous + additive (ethylene glycol, NaCl or NaSal) solution) has been studied using conductometry (at different temperatures), tensiometry, fluorescence and  $^1\text{H}$  NMR. The results are compared with their single tail counterparts. The temperature dependence of cmc and degree of counter ion dissociation ( $\alpha$ ) are used to compute various thermodynamic parameters. Tensiometry data has also been used to determine surface parameters ( $A_{\min}$ ,  $\Gamma_{\max}$ ,  $\pi_{\text{cmc}}$ ,  $\gamma_{\text{cmc}}$ ,  $\text{p}C_{20}$ ,  $\text{cmc}/C_{20}$ ). Micelle aggregation number ( $N_{\text{agg}}$ ) and micro-polarity of the individual micellar systems are also calculated from steady-state fluorescence quenching (SSFQ). 2D NOESY NMR spectroscopy has been performed to draw information related to interaction between spacer and alkyl tail of the gemini surfactant ( $m = 12$  or  $14$ ) well above their cmc ( $1.5$  to  $2.5 \times \text{cmc}$ ). A few DLS data are also collected to have an idea about size of the micelle at these concentrations.

## **3.2. Materials and Methods**

### **3.2.1. Materials**

Dodecyltrimethylammonium bromide (DTAB, 99%, TCI Chemicals), tetradecyltrimethylammonium bromide (TTAB, 99%, TCI Chemicals), cetyltrimethylammonium bromide (CTAB, 99%, Sigma Aldrich), pyrene (99%, Sigma Aldrich), cetylpyridiniumchloride (CPC, 99%, Sigma Aldrich) were used as received. Sodium chloride (NaCl, 99.5%, Merck) and sodium salicylate (NaSal, 99.5%, Merck) were dried in vacuum oven for 3 – 4 h before use. Absolute ethanol (99.6% v/v) dried over the activated Mg and I<sub>2</sub> (dried ethanol stored in moisture free environment). Dichloromethane (DCM, 99.5%, Merck) and dry ethylacetate (99.5%, S.D. Fine Chemicals) used as received. D<sub>2</sub>O (99.9%, Sigma Aldrich) and Norell 5 mm NMR tube have been used for <sup>1</sup>H NMR and 2D NOESY study and kept in a moisture free environment (in acrylic box with continuous N<sub>2</sub> supply). Water has been demineralized in appropriate KMnO<sub>4</sub> and KOH solution and double distilled in an all glass fit assembly. The specific conductivity of distilled water was 1-2 μS·cm<sup>-1</sup>.

### **3.2.2. Methods**

#### **3.2.2.1. Electrical Conductivity Measurements**

Conductometric measurements were performed by using a conductivity meter (EUTECH cyberscan CON510, cell constant 1 cm<sup>-1</sup>) with an inbuilt temperature sensor to obtain the critical micelle concentration (cmc) of gemini and conventional surfactants. A pre-calibrated (calibration done by 100 μS/cm KCl NIST traceable standard solutions) conductivity cell was used to obtain a specific conductance (κ) at

relevant concentration range. The stated uncertainty of the measurements was  $\pm 0.01 \mu\text{S}\cdot\text{cm}^{-1}$ . All the experiments were carried out in a water bath (SCHOTT CT1650) with an accuracy of  $\pm 0.05 \text{ K}$ . The cell dipped in 30 ml of distilled water (in glass vessel) was placed in a thermostat for at least 30 minutes before the addition of stock solution of gemini surfactant. A known volume of stock solution (500  $\mu\text{l}$ ) was then added to the water by microliter syringe and the solution was mixed carefully (with the help of cell). The conductance measurements were also repeated at different temperatures (283 to 323 K) to obtain the values of cmc, degree of micellar ionization ( $\alpha$ ) and various thermodynamic parameters. cmc and  $\alpha$  were determined from the intersection and ratio of the slopes of two straight lines in a plot of specific conductance ( $\kappa$ ) vs [surfactant], respectively [3].

Another significant parameter, Krafft temperature ( $T_k$ ), of all surfactants is also evaluated by same conductivity meter. Generally, various methods are reported to obtain  $T_k$  of the surfactant systems [29]. A modified method is adopted to obtain  $T_k$  in the present case. Here, 15 ml double distilled water has been cooled up to 273 K and then 1% solid surfactant was added. Conductivity measurements have been performed with gradual increase in temperature. The value of  $T_k$  has been obtained from the intersection point in a plot of  $\kappa$  vs temperature (Figure 1).

### **3.2.2.2. Fluorescence Measurements**

Fluorescence measurements have been carried out on a Jasco 4500 fluorescence spectrophotometer using 1 cm quartz cell at  $298 \pm 0.5 \text{ K}$ . Pyrene (2  $\mu\text{M}$ ) and CPC (between 0 and 0.05 mM) were employed as probe and quencher, respectively, in aqueous solution of surfactant, respectively. Concentrations of probe and quencher were low enough to avoid the possibility of “excimer formation” and to

ensure “poison distribution” [30]. The intensity was recorded with fixed excitation at 337 nm, and the slit widths of excitation and emission were fixed at 2.5 nm each. The emission spectra were scanned between 350-410 nm at a scan rate of 500 nm·min<sup>-1</sup>. The first vibration peak ( $I_1$ , 373 nm) and its ratio with third vibration peak ( $I_3$ , 384 nm) in the fluorescence spectra has been used to evaluate the  $N_{agg}$  / polarity of the environment and cmc of the surfactant [30]. Micelle aggregation number,  $N_{agg}$ , was calculated from the slope of the linear plot between  $\ln(I_o/I_q)$  vs [Q] using following equations [32],

$$\ln\left(\frac{I_o}{I_q}\right) = \frac{N_{agg}C_q}{C_s - cmc} \quad (1)$$

where,  $I_q$  and  $I_o$  are the fluorescence intensities of pyrene in the absence and presence of the quencher (CPC) at a wavelength of 374 nm,  $C_q$ ,  $C_s$  and  $C_m$  are the molar concentrations of the quencher, total surfactant concentration and micellar concentration, respectively.

### 3.2.2.3. <sup>1</sup>H NMR and 2D NOESY Spectroscopy

Sample of gemini surfactant in D<sub>2</sub>O has been individually prepared in volumetric flask below and above their cmc and then syringe out in to the NMR tube. <sup>1</sup>H NMR experiments were carried out on a Bruker NMR spectrometer with a proton resonance frequency of 400.15 MHz in D<sub>2</sub>O at 298 K. The acquisition and analysis of spectra were done by TOPSIN-13 software. The HOD signal (4.790 ppm) used as a reference for proton chemical shifts, which remained constant throughout. The number of scan remains constant (16) to achieve good signal to noise ratio. The centre of the HOD ( $\delta = 4.26$  ppm) signal was used as a reference in D<sub>2</sub>O (HOD peak is not display) solutions. The two-dimensional nuclear Overhauser enhancement

spectroscopy (2D NOESY) and correlation spectroscopy (2D COSY) experiments are performed above the cmc (1.5 x cmc). The data are acquired with a standard pulse programme with a 16 NS (net scans) and 4 DS (dummy scans).

#### **3.2.2.4. Particle Size Measurements**

Particle size measurements have been obtained by dynamic light scattering measurements on a Brookhaven 90 plus spectrometer equipped with a built in temperature controller ( $\pm 0.5^\circ\text{C}$ ). Light of  $\lambda$  of 633 nm from 15 mW solid state He-Ne laser was used as the incident beam with  $90^\circ$  scattering angle and the intensity autocorrelation functions were analyzed by using the methods of Cumulant and non-negatively constrained least-squares (NNLS) algorithm. The hydrodynamic diameter ( $D_h$ ) was calculated according to Stokes-Einstein equation,  $D_h = k_B T / (3\pi\eta D)$  where,  $D$  is diffusion coefficient,  $k_B$  is the Boltzmann constant,  $T$  is the absolute temperature, and  $\eta$  is the solvent viscosity. For particle size measurements, solution was filtered through 0.22  $\mu\text{m}$  nylon membrane filter (to remove dust or foreign particles) and then directly transferred into the 10 mm plastic cuvette. Sample cuvette was placed in the sample chamber 15 min before prior the measurement. The data obtained in each case are the average of 10 runs, each run of 30s duration.

### 3.3. Results and Discussion

#### 3.3.1. Aqueous Solubility of Gemini Surfactants

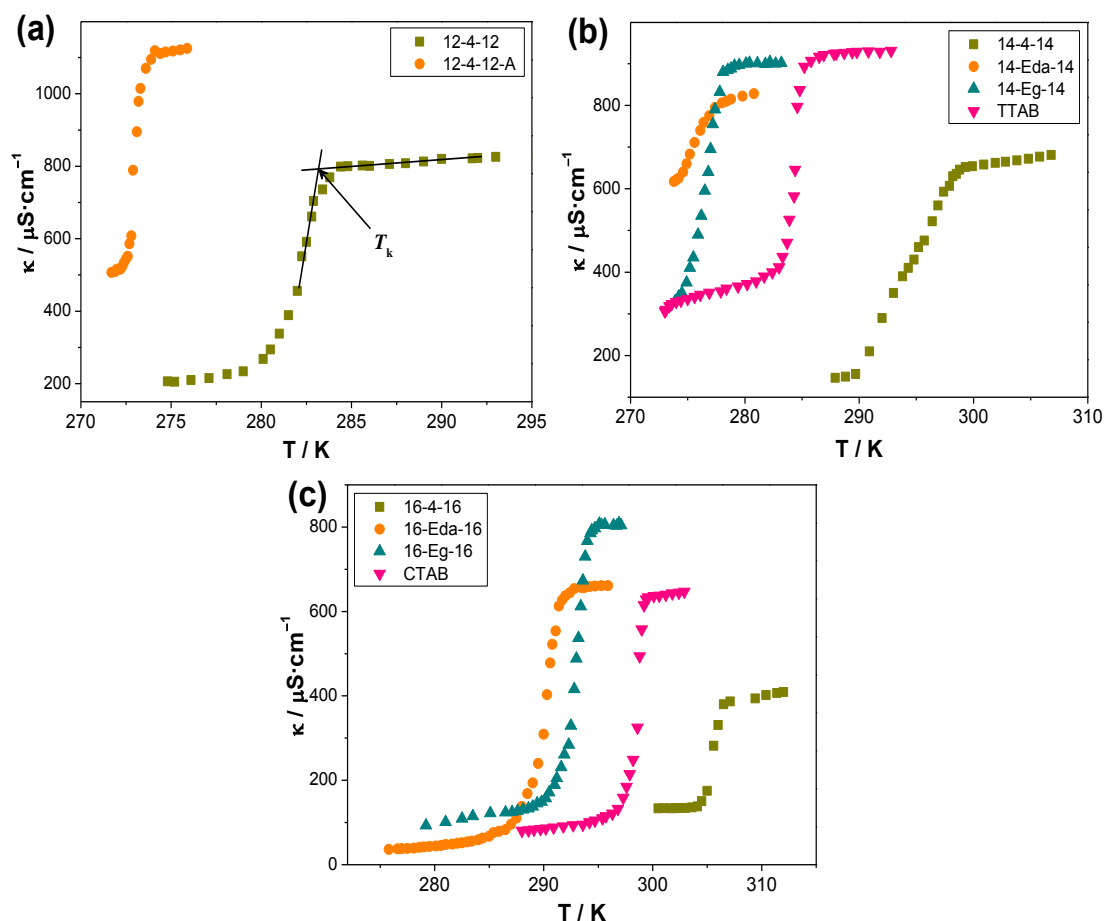


**Figure 1.** Plot of specific conductance ( $\kappa$ ) vs temperature (K) to obtain Krafft temperature ( $T_k$ ) of: (a) 12 series anionic and cationic geminis; (b) 14 series cationic conventional and geminis; (c) 16 series cationic conventional and geminis.

The most basic requirement of any surfactant after its syntheses is to check its aqueous solubility. It has been checked by conductometry of aqueous surfactant solution (1% w/v) by gradual increase in temperature. In Figure 1a, maximum solubility of surfactant has been obtained by the break point. That break point denotes the Krafft temperature ( $T_k$ ). All gemini and conventional surfactants aqueous solubility plots are shown in Figure 1. Aqueous solubility of anionic gemini surfactant

(12-4-12-A) has also been checked for comparison. A few surfactants were easily solubilize even at freezing temperature of water ( $\sim 273$  K).

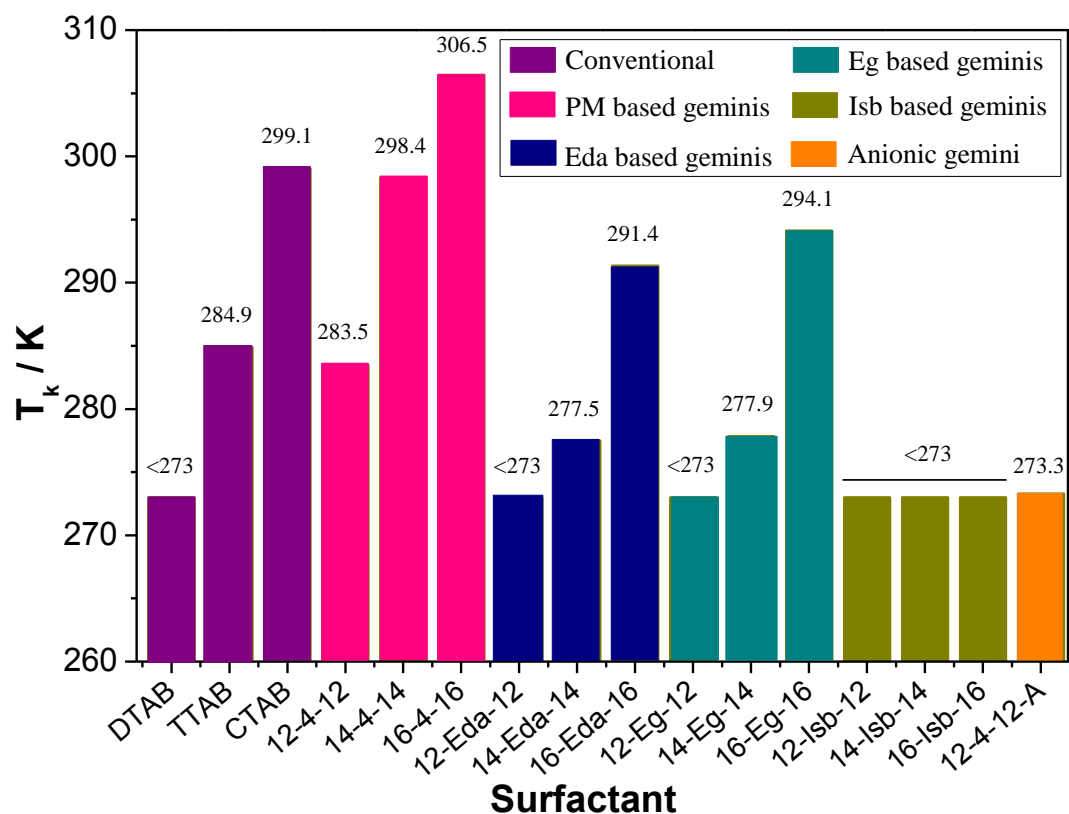


**Figure 2.** Representative plot of Krafft temperature ( $T_k$ , K) vs all surfactants (conventional and geminis).

$T_k$  values of all surfactants are depicted in Figure 2. Biocompatible spacer based geminis have lower  $T_k$  values than polymethylene spacer containing surfactants. This may be due to two reasons: (a) the replacement of  $\text{Br}^-$  by  $\text{Cl}^-$  [32] and (b) additional hydration at the surface of micelle due to the presence of “O” atoms. However, the general trend of  $T_k$  variation with increasing  $m$  remained similar for all the surfactants (except  $m$ -Isb- $m$ ). Within biocompatible spacers, isosorbide spacer based geminis have even better aqueous solubility ( $<273$  K). This was mainly due to the highly hygroscopic nature (due to presence of more “O” atoms) of isosorbide moiety [33]. Therefore, isosorbide spacer based gemini surfactant could be a good candidate for wide temperature range applications. Anionic gemini surfactant (12-4-

12-A) also shows better aqueous solubility (273.3 K) than 12-4-12. This confirms that head group can also play a crucial role in aqueous solubility of surfactant.  $T_k$  values of conventional and polymethylene geminis have been found in good agreement with literature values [32] which validate the measurement.

### 3.3.2. Micellization of Gemini Surfactants

Physical properties of aqueous surfactant solution vary with two different rates before and after micellization. To determine cmc, different methods (like, conductometry, calorimetry, tensiometry,  $^1\text{H}$  NMR, specific rotation, fluorescence, UV spectroscopy, etc.) have been used earlier [34]. Four methods (conductometry, tensiometry, fluorescence and  $^1\text{H}$  NMR) are used to obtain micellization data (micelle formation at particular concentration range) of synthesized cationic gemini as well as conventional surfactants. Additionally, micellization of anionic gemini surfactant (12-4-12-A) has also been studied by above techniques (except  $^1\text{H}$  NMR) for comparison purposes.

#### *Micellization by Conductometry*

Conductivity measurement is one of the most widely used methods for obtaining the change in micellization. As increased the [surfactant], conductance was first gradually increased up to certain concentration then after it will steep decreased. At certain, the sharp / narrow break point was obtained, which allow us to identify the critical micelle concentration (cmc) precisely. Representative plots of specific conductance ( $\kappa$ ) vs [surfactant] of cationic conventional and all synthesized cationic and anionic gemini surfactants are shown in Figure 3 at 298 K. The cmc data of all surfactants are compiled in the Table 2.

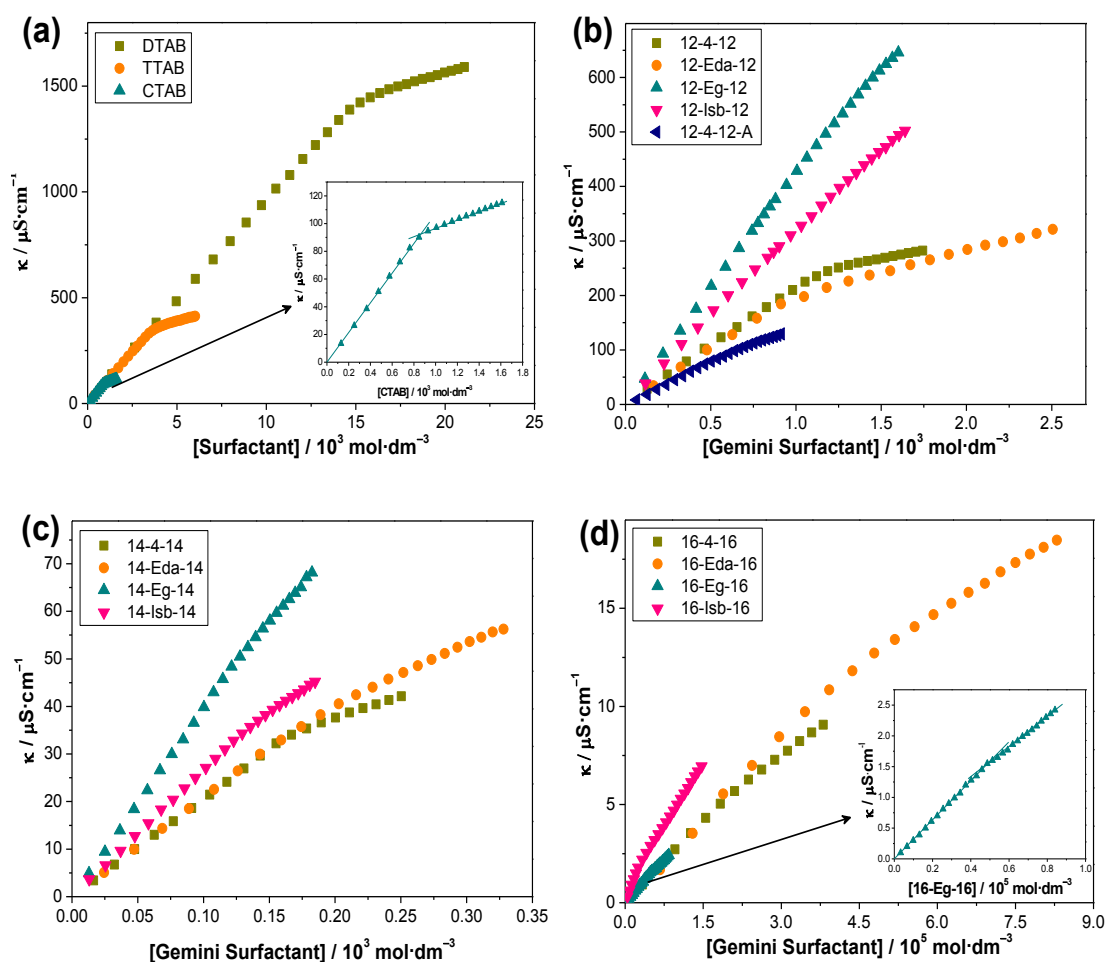


**Figure 3.** Plot of specific conductance ( $\kappa$ ) vs concentration of cationic conventional (a) and gemini surfactants with biocompatible and polymethylene spacers in aqueous solution at 298 K: (b)  $m = 12$ ; (c)  $m = 14$ ; (d)  $m = 16$ .

The degree of micellar ionization ( $\alpha$ ) for conventional and gemini surfactants are also obtained from the same conductivity plot ( $\kappa$  vs [surfactants]) by using the ratio of the slopes of two straight lines (Figure 3). The values of  $\alpha$  for all surfactants were summarized in Table 1. It has been observed that  $\alpha$  values of geminis are higher than the conventional surfactants. geminis have the larger area per head group compared to conventional and, hence, responsible for the larger value of  $\alpha$ . The values of  $\alpha$  within geminis were found higher for  $\text{Cl}^-$  ( $m$ -Eda- $m$ ,  $m$ -Eg- $m$ ,  $m$ -Isb- $m$ ) than  $\text{Br}^-$  ( $m$ -4- $m$ ), which indicates less binding of chloride counter-ions to head group. The  $\alpha$  of ester and isosorbide spacer based geminis were even higher than the amide

spacer based geminis, which may be due to higher hydration of micelle surface. With increasing the  $m$ , micellar ionization have been found increasing for  $m$ -4- $m$ ,  $m$ -Eg- $m$  and  $m$ -Isb- $m$ . However, there is no such trend with  $m$ -Eda- $m$ .

**Table 1.** Degree of micellar ionization of conventional and gemini surfactants in aqueous solution at 298 K.

Surfactants	Degree of micellar Ionization ( $\alpha$ )		
	12 series	14 series	16 series
$C_m$ TAB	0.28	0.26	0.28
	0.28 <sup>b</sup>	0.23 <sup>d</sup>	0.29 <sup>a</sup>
$m$ -4- $m$	0.28	0.47	0.69
	0.24 <sup>c</sup>	0.34 <sup>c</sup>	0.64 <sup>a</sup>
$m$ -Eda- $m$	0.40	0.61	0.59
$m$ -Eg- $m$	0.89	0.79	0.72
$m$ -Isb- $m$	0.89	0.72	0.63

<sup>a,b,c,d</sup> data used as such from [2, 35a, 26, 35b and 23], respectively.

### *Micellization by Tensiometry*

The surface tension measurement is a classical method of studying not only the micellization but also for the purity of the newly synthesized surfactants. The variation of the surface tension ( $\gamma$ ) with the surfactant concentration ( $\log C$ , where  $C$  is the surfactant molar concentration) is shown in Figure 4. Surface tension remained same after each break denotes the micelle forming point, which allows to obtain cmc precisely. The obtained cmc values of all surfactants are tabulated in the Table 2.

The absence of minima (near the break point) in the surface tension plot (Figure 4) is also indicative of the purity. In addition, the surface parameters are also obtained from the same plot (Figure 4), and data are compiled in Table 3.

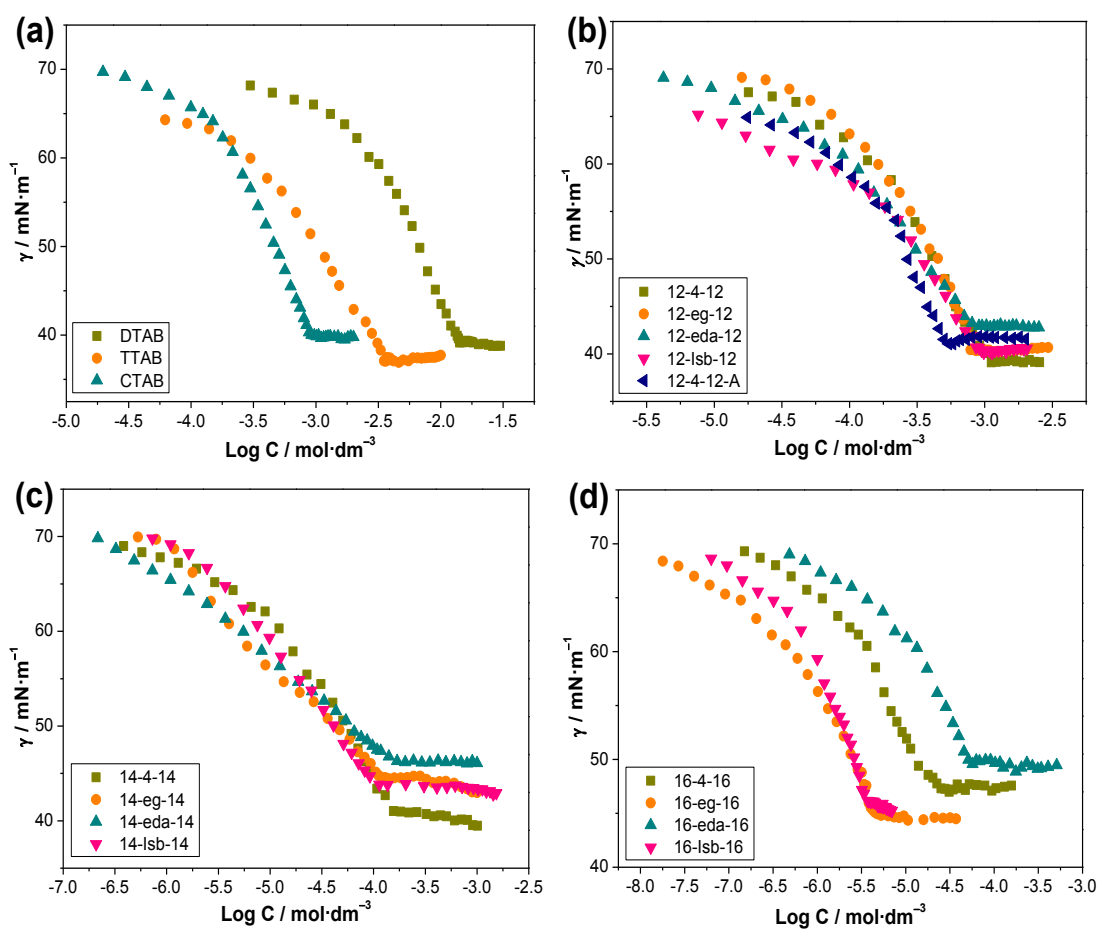


**Figure 4.** Variation of surface tension ( $\gamma$ ) with the log of gemini and conventional surfactants concentration ( $C$ ) in aqueous solution at 303 K.

#### *Micellization by Fluorescence Measurements*

Pyrene is often used as probe to investigate the micellization in surfactant solution [34a]. Generally, pyrene gives four (I, II, III and IV) vibrational peaks (see Figure 5) in aqueous solution under the exposure of photo luminescence (fluorescence). In fluorescence measurement, at desired [surfactant] (Figure 5), most of the changes have been observed in the 3<sup>rd</sup> vibrational peak of pyrene (2  $\mu\text{M}$ ) above and below cmc due to its site of solubilization, polarity and microenvironment [36]. Micellization can easily be identified from the intensities ratio of I to III vibration peaks ( $I_1/I_3$ ). Representative pyrene fluorescence emission spectra are shown in Figure 5.

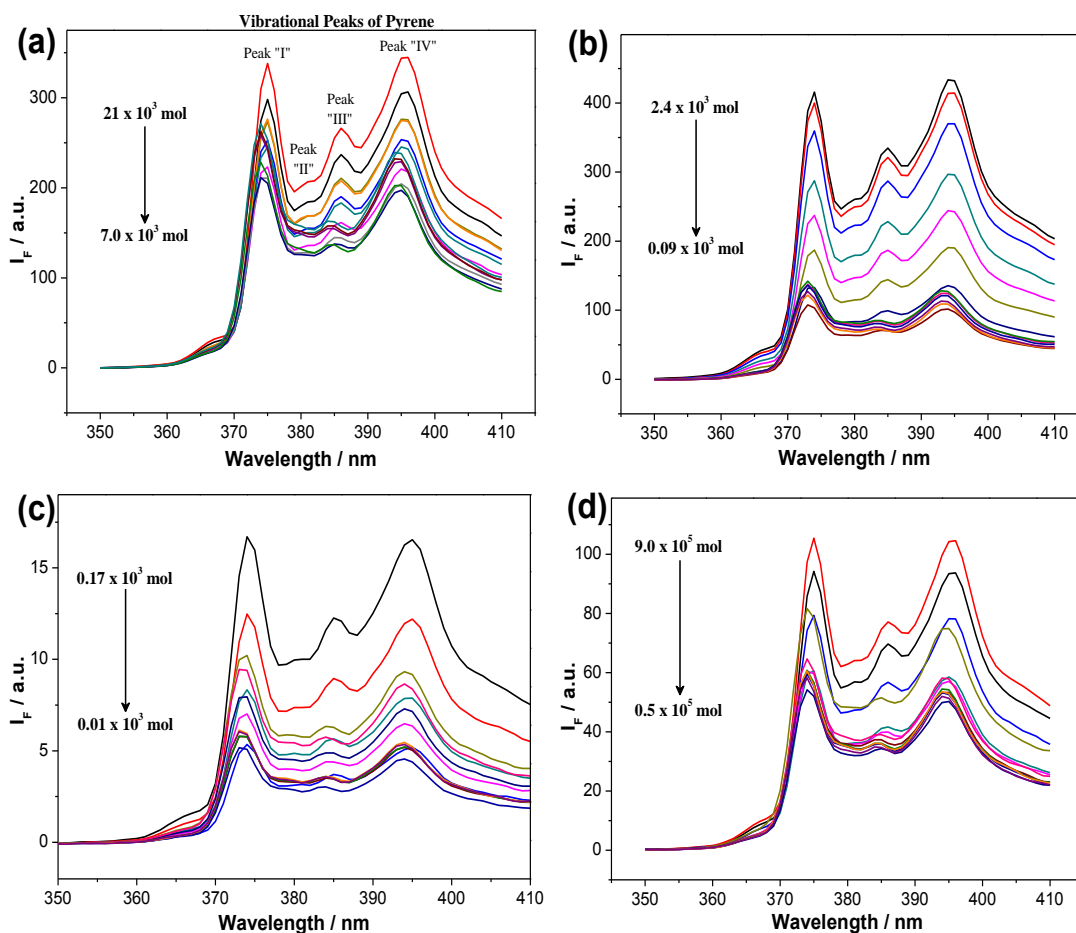


**Figure 5.** Representative Fluorescence (emission) spectra of  $2\mu\text{M}$  pyrene in aqueous solution of (a) DTAB; (b) 12-Eg-12; (c) 14-Isb-14; (d) 16-4-16.

The plot of  $I_1 / I_3$  vs [surfactant] gives the cmc (Figure 6). The cmc data of all conventional and gemini surfactants are also displayed in Table 2. After cmc, value of intensity ratio ( $I_1 / I_3$ ), generally, remain constant due to compactness of the micelle (except 16-Eda-16). In case of 16-Eda-16,  $I_1 / I_3$  show a decrease (though with less change) with increasing concentration even after cmc. This indicates about the looseness of micelle formed by 16-Eda-16. Higher hydrophilicity of the spacer may have role to increases the steric hindrance of surfactant molecule in the self assembly [37]. However, micellization of 16-Eg-16 and 16-Isb-16 geminis have not been obtained by fluorescence measurement. This may be due comparable value of cmc and [pyrene].

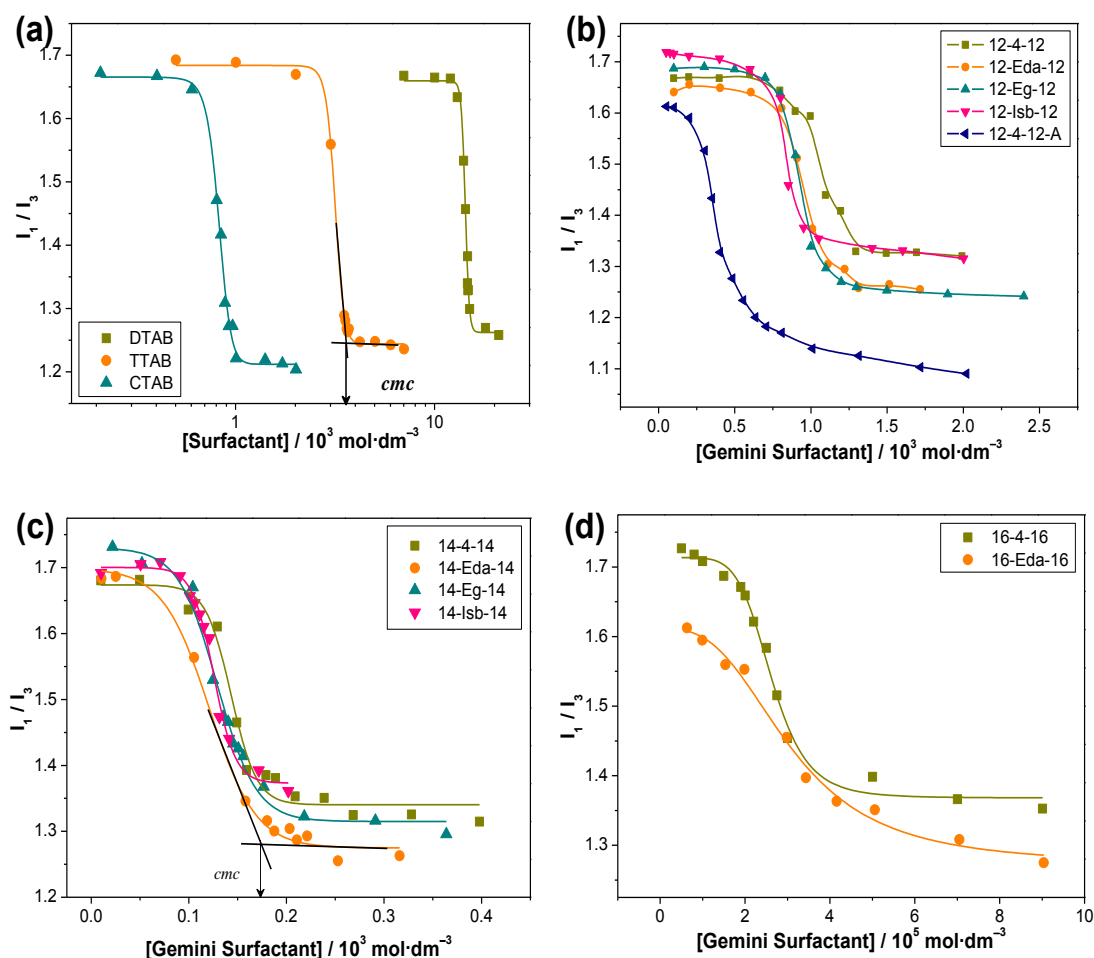


**Figure 6.** Plot of  $I_1/I_3$  (ratio of vibrational peaks of pyrene) vs [surfactants] at 298 K: (a) conventional surfactants; geminis with (b)  $m = 12$ ; (c)  $m = 14$ ; (d)  $m = 16$ .

### Micellization by $^1\text{H}$ NMR

Since the chemical shifts of protons in a surfactant molecule are very sensitive to the medium polarity and molecular conformation [38]. As an accurate and sensitive method,  $^1\text{H}$  NMR (chemical shift of protons) has also been used for micelle formation in recent past [39]. Chemical shifts ( $\delta$ ) reflect the next / nearest neighboring environment of the protons which can be used to know about surface and palisade layer of the aggregate. There are only a few studies on micellization of gemini surfactants using  $^1\text{H}$  NMR [38, 40].

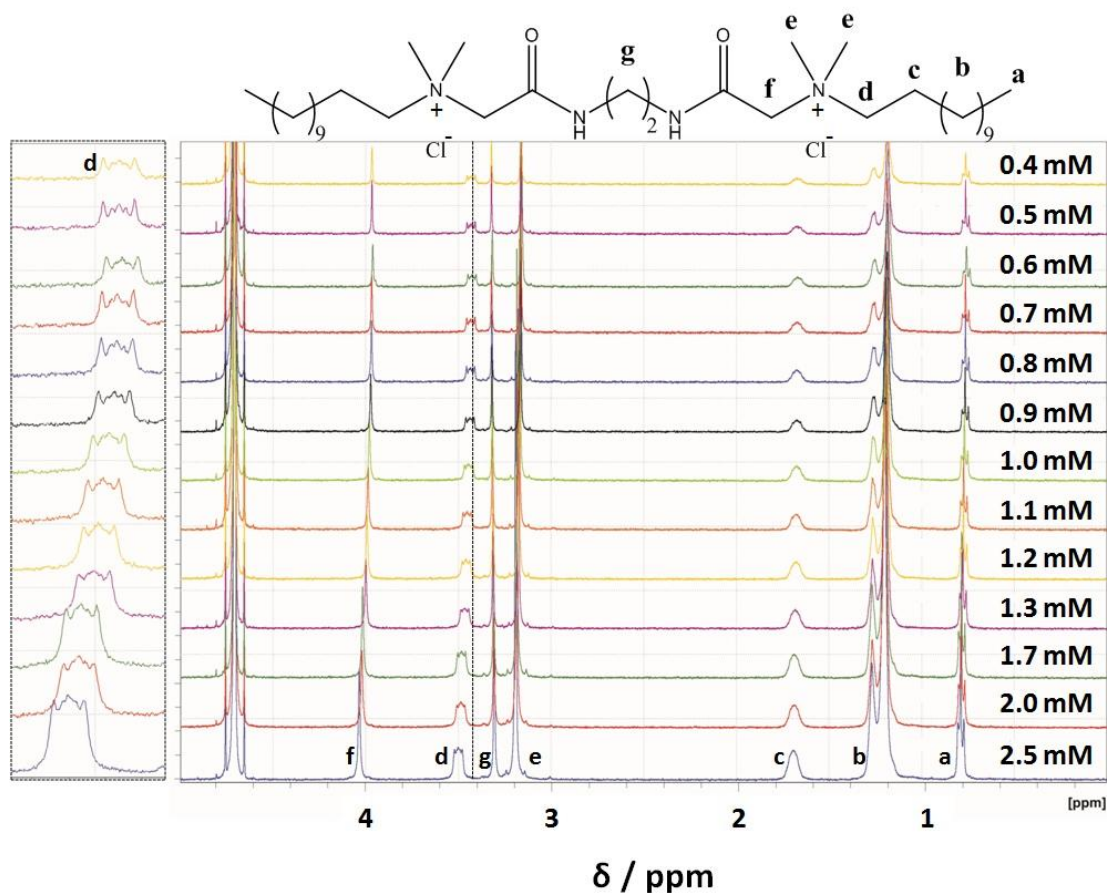


**Figure 7.** Representative spectra of  $^1\text{H}$  NMR and their proton assignment with chemical structure of 12-Eda-12 in  $\text{D}_2\text{O}$  at different concentrations (below and above micellization).

Here, for the purpose, cationic gemini surfactants (with  $m = 12$ ) has been used (with a concentration range from  $\sim 0.4$  mM to  $\sim 3.0$  mM) to examine the  $\delta$  changes. Micellization studies for other geminis (14 and 16 series) are hampered due to relatively lower cmc. Figure 7 shows representative proton peaks of 12-Eda-12 below and above micellization in  $\text{D}_2\text{O}$ . The  $\delta$ -values of all signals are found identical up to certain concentration and then a downfield shift observed (except proton  $\text{H}_g$  of 12-Eda-12 which shows up field). The  $\alpha\text{-CH}_2$  ( $\text{H}_d$ ) of alkyl chain of all surfactants has been used to determine the cmc under the fast exchange in most of the studies [39c, 41]. Therefore, after obtaining the values of  $\alpha\text{-CH}_2$  proton ( $\text{H}_d$ ) of geminis,  $\delta$  was plotted against the concentration of surfactants (Figure 8a). The variations of chemical

shifts with [gemiins] are showing a breakpoint of two straight lines, which provides the cmc and chemical shift at cmc ( $\delta_{\text{cmc}}$ ). These values of cmc are also listed in Table 2.

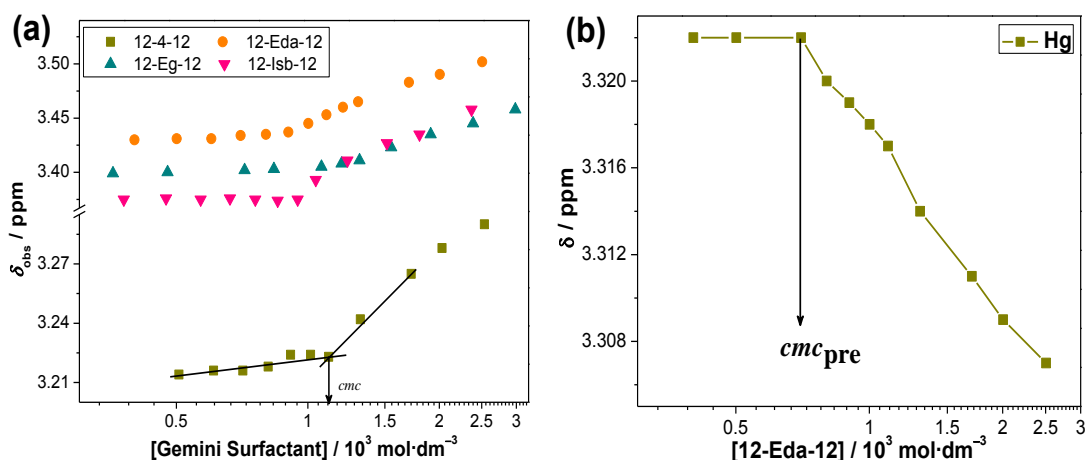


**Figure 8.** (a) Representative plot of  $\delta_{\text{obs}}$  (obtained from  $^1\text{H}$  NMR chemical shift of the proton “d”,  $\text{H}_d$ ) vs [gemini surfactant] in  $\text{D}_2\text{O}$  at 298 K. (b) Variation of chemical shift ( $\delta$ ) “g” proton ( $\text{H}_g$ ) of 12-Eda-12 in  $\text{D}_2\text{O}$ .

Interestingly, only proton ( $\text{H}_g$ ) of 12-Eda-12 (Figure 8b) shows up field shift even below the cmc (up to 0.7 mM), indicating hydration of the spacer proton ( $\text{H}_g$ ). This may be due to pre-micellization ( $\text{cmc}_{\text{pre}}$ , formation of loose micelles below conventional cmc) of monomers. These observations are hinting towards a stepwise association. The abrupt change (up field and downfield) of chemical shifts may be due to the two reasons: medium and conformation effects [42]. The medium effect is attributed to the removal of polarity (in form of  $\text{D}_2\text{O}$  and H-bonding) from the system which leads the downfield shift (*vide supra*) [43]. In other effect, micelle formation is the results of changeover from gauche to trans conformation state of alkyl chains which also contributes to the downfield shift [42a, 44]. The  $\delta_{\text{cmc}}$  values indicate the polarity of micellar environment at cmc ( $\delta$  values are 3.22 (12-4-12), 3.44 (12-Eda-12), 3.41 (12-Eg-12) and 3.38 (12-Isb-12)). 12-Eda-12 was produces relatively a polar micelle at cmc (and even blow and above cmc, Figure 8a).

### *Comparison of cmc Values by Different Techniques*

All techniques gave nearly similar cmc values with narrow concentration range (Table 2) which indicate the validity of the measurement. However, a little variation in cmc values is mainly due to the nature of the technique and its response to the phenomenon (here surface tension is mainly sensitive to the concentration of the monomeric form as micelles are non surface active, electrical conductivity depends on the mobilitites of all the ionic species, fluorescence mainly depends on the solubilization sites of the probe while  $^1\text{H}$  NMR signals are dependent on proton environment and its polarity) [45]. The cmc values of gemini surfactants are found one order of magnitude lower than their conventional counterparts (Table 2). Table 2 also contains the cmc data available in literature for conventional and geminis ( $s =$  polymethylene). cmc data are in fair agreement with the literature values [2, 26, 35b, 46, 47].

The cmc data follows a trend, where, it decreases with the hydrophilicity / polarity of the geminis surfactants increases. In an earlier study [48], it has been pointed out that hydrophilic spacer can easily be located at the micelle-water interface and, therefore, can be in hydrated form. This results in reduction of the coulombic repulsive interactions between the head groups. The geminis (with biocompatible spacers) are showing similar trend as the hydrophilicity increases. Anionic gemini (12-4-12-A) has even lower cmc than the cationic gemini (12-4-12), indicating that head group and nature of charge can also play a role micellization. However, a cmc decrease with increasing  $m$  has been noticed as reported in other studies [32].

**Table 2.** Critical micelle concentration (cmc) of all conventional and gemini surfactants in aqueous solution at desired temperature ( $T$ ) by different techniques.

Surfactants	cmc / mol·dm <sup>-3</sup>			
	Conductometry <sup>a</sup>	Tensiometry <sup>b</sup>	Fluorescence <sup>a</sup>	<sup>1</sup> H NMR <sup>c</sup>
DTAB	1.47 × 10 <sup>-2</sup> (1.48 × 10 <sup>-2</sup> ) <sup>d</sup>	1.43 × 10 <sup>-2</sup> (1.47 × 10 <sup>-2</sup> ) <sup>d</sup>	1.48 × 10 <sup>-2</sup>	-
TTAB	3.62 × 10 <sup>-3</sup> (3.56 × 10 <sup>-3</sup> ) <sup>e</sup>	3.75 × 10 <sup>-3</sup>	3.58 × 10 <sup>-3</sup> (3.50 × 10 <sup>-3</sup> ) <sup>h</sup>	-
CTAB	8.70 × 10 <sup>-4</sup> (9.25 × 10 <sup>-4</sup> ) <sup>f</sup>	9.35 × 10 <sup>-4</sup>	9.46 × 10 <sup>-4</sup>	-
12-4-12	1.12 × 10 <sup>-3</sup> (1.14 × 10 <sup>-3</sup> ) <sup>d</sup>	1.10 × 10 <sup>-3</sup> (1.03 × 10 <sup>-3</sup> ) <sup>d</sup>	1.25 × 10 <sup>-3</sup>	1.12 × 10 <sup>-3</sup>
14-4-14	1.80 × 10 <sup>-4</sup> (1.40 × 10 <sup>-4</sup> ) <sup>e</sup>	1.51 × 10 <sup>-4</sup>	1.68 × 10 <sup>-4</sup>	-
16-4-16	2.44 × 10 <sup>-5</sup> (2.70 × 10 <sup>-5</sup> ) <sup>g</sup>	2.15 × 10 <sup>-5</sup>	2.97 × 10 <sup>-5</sup>	-
12-Eda-12	1.04 × 10 <sup>-3</sup>	9.07 × 10 <sup>-4</sup>	1.09 × 10 <sup>-3</sup>	9.03 × 10 <sup>-4</sup>
14-Eda-14	2.00 × 10 <sup>-4</sup>	1.60 × 10 <sup>-4</sup>	1.73 × 10 <sup>-4</sup>	-
16-Eda-16	4.38 × 10 <sup>-5</sup>	4.77 × 10 <sup>-5</sup>	4.60 × 10 <sup>-5</sup>	-
12-Eg-12	8.39 × 10 <sup>-4</sup>	7.90 × 10 <sup>-4</sup>	1.03 × 10 <sup>-3</sup>	9.75 × 10 <sup>-4</sup>
14-Eg-14	1.20 × 10 <sup>-4</sup>	1.12 × 10 <sup>-4</sup>	1.54 × 10 <sup>-4</sup>	-
16-Eg-16	3.40 × 10 <sup>-6</sup>	4.25 × 10 <sup>-6</sup>	-	-
12-Isb-12	8.26 × 10 <sup>-4</sup>	8.59 × 10 <sup>-4</sup>	9.25 × 10 <sup>-4</sup>	9.46 × 10 <sup>-4</sup>
14-Isb-14	1.13 × 10 <sup>-4</sup>	1.08 × 10 <sup>-4</sup>	1.35 × 10 <sup>-4</sup>	-
16-Isb-16	2.70 × 10 <sup>-6</sup>	3.54 × 10 <sup>-6</sup>	-	-
12-4-12-A	5.31 × 10 <sup>-4</sup>	4.97 × 10 <sup>-4</sup>	5.20 × 10 <sup>-4</sup>	-

<sup>a, b</sup> and <sup>c</sup> temperature is respectively 298, 303 and 293 K. <sup>d, e, f, g, h</sup> data used such from [35a], [49], [35b], [46], [34a], respectively.

### 3.3.3. Surface Parameter of Gemini Surfactants

Surface parameters ( $\gamma_{\text{cmc}}$ , the  $pC_{20}$  (negative logarithm of  $C_{20}$ , concentration of surfactant required to lower the surface tension of water ( $\gamma_o$ ) by 20 mN/m),  $\text{cmc}/C_{20}$  ratio and surface pressure at the cmc ( $\pi_{\text{cmc}}$ ) have also been computed from  $\gamma$  vs  $\log C$  plot (Figure 4) by using following equations,

$$pC_{20} = -\log C_{20} \quad (2)$$

$$\pi_{cmc} = \gamma_o - \gamma_{cmc} \quad (3)$$

Surface tension at the cmc ( $\gamma_{cmc}$ ) values were obtained (from Figure 4) and listed in Table 3.

**Table 3.** Surface parameters of gemini surfactants as determined from surface tension measurements in aqueous solution at 303 K.

Surfactants	$\gamma_{cmc}$ mN·m <sup>-1</sup>	$\Gamma_{max}$ 10 <sup>6</sup> mol·m <sup>-2</sup>	$A_{min}$ nm <sup>2</sup>	pC <sub>20</sub>	$\pi_{cmc}$ mN·m <sup>-1</sup>	cmc/C <sub>20</sub>
DTAB	39.24	2.92 (1.95)	0.57 (0.85)	2.17	28.96	2.13
TTAB	36.89	2.00 (1.33)	0.83 (1.25)	2.98	28.51	3.56
CTAB	39.72	3.02 (2.02)	0.55 (0.82)	3.33	31.88	1.99
12-4-12	39.11	2.27 (1.52)	0.73 (1.10)	3.38	29.14	2.66
14-4-14	41.01	1.69 (1.13)	0.98 (1.47)	4.27	28.89	0.90
16-4-16	47.20	1.62 (1.08)	1.02 (1.54)	4.90	22.60	1.69
12-Eg-12	40.40	2.78 (1.85)	0.60 (0.90)	3.35	30.60	1.77
14-Eg-14	44.74	0.96 (0.64)	1.74 (2.61)	4.37	25.71	2.60
16-Eg-16	44.80	1.76 (1.17)	0.95 (1.42)	5.60	23.90	1.68
12-Eda-12	42.79	1.68 (1.12)	0.99 (1.48)	3.47	26.86	2.64
14-Eda-14	46.13	0.80 (0.54)	2.07 (3.10)	4.22	23.97	2.64
16-Eda-16	50.02	1.57 (1.02)	1.06 (1.63)	4.43	20.08	1.27
12-Isb-12	40.24	1.97 (1.31)	0.84 (1.26)	3.47	30.73	2.53
14-Isb-14	43.46	1.20 (0.80)	1.38 (2.07)	4.38	26.54	1.61
16-Isb-16	46.22	1.10 (0.67)	1.51 (2.46)	5.53	22.45	1.35
12-4-12-A	41.16	2.97 (1.98)	0.56 (0.84)	3.57	29.43	1.85

$\gamma_{cmc}$ , surface tension at the cmc;  $\Gamma_{max}$ , maximum surface excess concentration;  $A_{min}$ , area per molecule at the interface;  $\pi_{cmc}$ , surface pressure at the cmc;  $C_{20}$ , surfactant concentration required to reduce the surface tension of the water by 20 mN/m. The values in parentheses are for n = 3.

$\gamma_{cmc}$  increases with the alkyl chain length ( $m$ ) except conventional surfactants.  $\pi_{cmc}$  decides surface activity of the surfactant. These parameters for all surfactants are also listed in Table 3. Data show that biocompatible spacer based geminis ( $m$ -Eda,Eg,Isb- $m$ ) have higher  $\gamma_{cmc}$  and lower  $\pi_{cmc}$  values compared to conventional and polymethylene spacer based geminis ( $m$ -4- $m$ ). This may be due to two factors: (a) protonated spacer will not bend (due to H-bonding) towards core and not extend to air

as compared to polymethylene spacer and (b) at the interface, arrangement of amphiphilic molecules may not be easy to adjust or giving a space to other amphiphiles with a bigger size protonated spacer [50]. However,  $\pi_{cmc}$  decreases with  $m$  which is in agreement with the earlier report [51]. Data revealed that the nature of the spacer can play an important role in the surface arrangements of the surfactant molecules. Lower  $\gamma_{cmc}$  and higher  $\pi_{cmc}$  values for anionic gemini surfactant (12-4-12-A) clearly suggests similar arrangements at interface as of cationic gemini (12-4-12). The larger value of  $pC_{20}$  denotes the higher adsorption efficiency of surfactant molecules and greater efficiency in reducing surface tension.  $pC_{20}$  value increases with the increase in size of hydrophobic tail ( $m$ ) indicating that the surfactant with higher  $m$  has better surface activity. The  $cmc/C_{20}$  ratio gives the idea of adsorption and micellization process at the air/water interface and in bulk, respectively. The values of  $cmc/C_{20}$  were found to be independent on  $s$  and  $m$ .

The packing densities at the air-water interface are important to interpret the surface activity of surfactants. Maximum surface excess quantity ( $\Gamma_{max}$ , in mole/m<sup>2</sup>) at the air/water interface can be calculated by applying the following Gibbs adsorption isotherm [52] (Eq. 4),

$$\Gamma_{max} = -\frac{1}{2.303nRT} \left( \frac{d\gamma}{d \log C} \right)_T \quad (4)$$

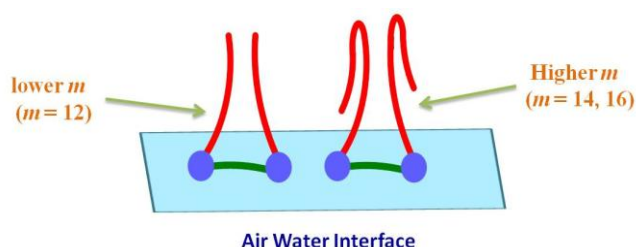
where,  $R$  is the gas constant (8.314 Jmol<sup>-1</sup>K<sup>-1</sup>),  $T$  is absolute temperature (303 K) and  $(d\gamma/ d\log C)_T$  is the slope of the line (below the cmc) in  $\gamma$  vs  $\log C$  plot. For conventional amphiphiles,  $n = 2$  is used [53]. In recent studies on geminis, the value of  $n$  was used either 2 or 3 [51b, 54]. It was argued that with gemini surfactant ions and counter-ion are univalent, therefore, the value  $n = 2$  should be used for calculating

surface excess concentration. In the present study (Table 3),  $\Gamma_{\max}$  for the all gemini as well as conventional surfactants is calculated with  $n = 2$  and  $n = 3$  (mentioned in parentheses).

The minimum area occupied per surfactant molecule ( $A_{\min}$ , in  $\text{nm}^2$ ) at air-water interface has been computed using following relation (Eq. 5),

$$A_{\min} = \frac{10^{18}}{N_A \Gamma_{\max}} \quad (5)$$

where,  $N_A$  is the Avogadro number ( $6.023 \times 10^{23} \text{ mol}^{-1}$ ).  $A_{\min}$  (Table 3) reflects the packing density of surfactant monomer at the air-water solution interface which is related to surface activity of the surfactant.



**Scheme 1.** Representation of gemini monomers arrangement the air-water interface.

The  $\Gamma_{\max}$  value decreases while the  $A_{\min}$  value increases with increase in  $m$  except geminis 14-Eg-14 and 14-Eda-14 suggesting that the surfactant with lower hydrophobicity has higher packing density at air/water interface. This is mainly due the fact that lower  $m$  chain may stand vertical to the surface and less prone to fold at the air/water interface (Scheme 1).  $A_{\min}$  value shows a trend:  $m\text{-Eg-}m < m\text{-Isb-}m < m\text{-4-}m < m\text{-Eda-}m$ . This may be due to the presence of more protonated (oxygenated) molecules in the spacer which allow the spacer to remain horizontal to the surface of water due to H-bonding and forcing alkyl chain to remain vertical to the surface causing lower value of  $A_{\min}$  for ester and isosorbide spacers. Therefore,  $m\text{-Eg-}m$  and

*m*-Isb-*m* have higher packing densities at the interface as well as in the bulk than the other ones.  $A_{\min}$  values of conventional surfactants found even lower compared to geminis due to tighter packing at the interface. Interestingly, 12-4-12-A (anionic gemini) has similar  $A_{\min}$  value to that of conventional ones suggesting that it has tighter packing density at the interface and bulk compared to 12-4-12. However, the use of different values of  $n$  (2 or 3) in calculating  $I_{\max}$  and  $A_{\min}$  do not affect much the computed results.

### 3.3.4. Aggregation Number ( $N_{\text{agg}}$ ) and Micro-polarity

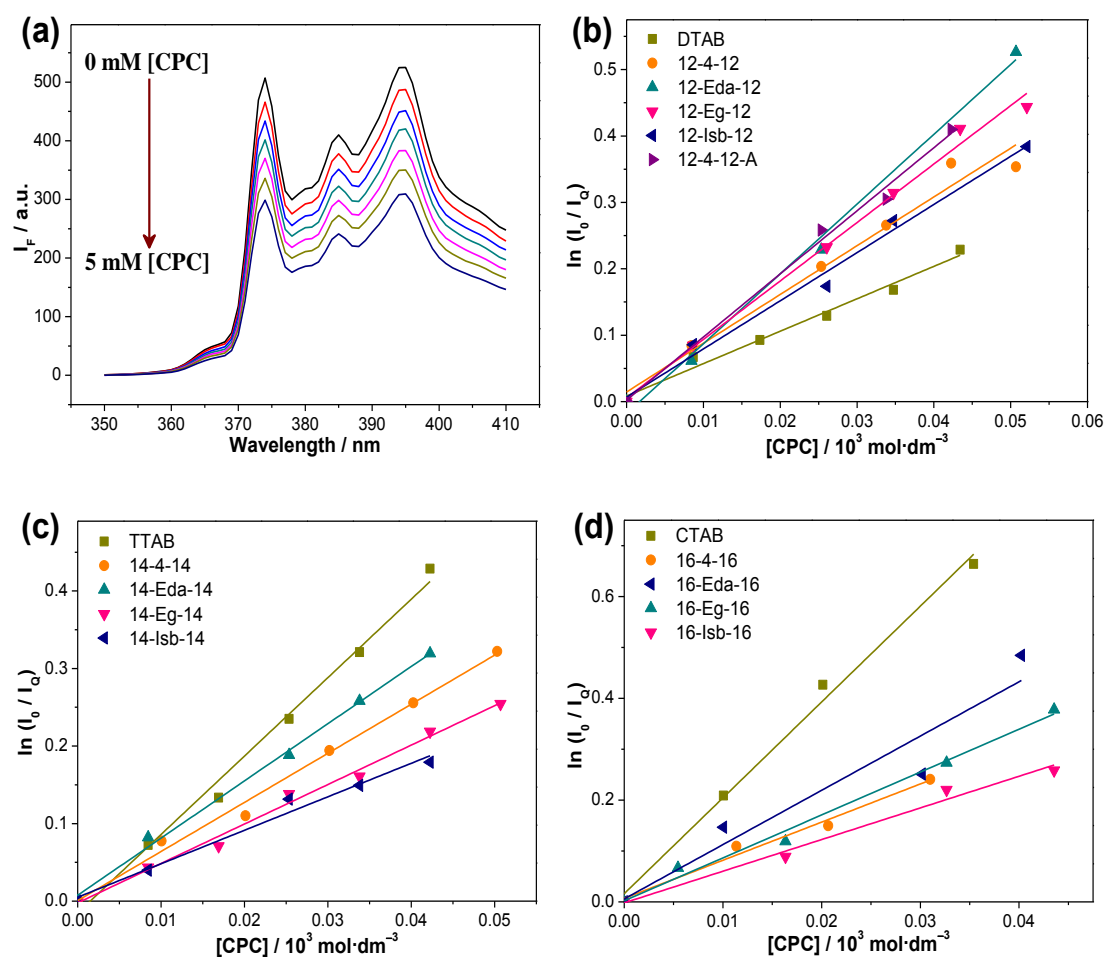


**Figure 9.** (a) Fluorescence (emission) spectra of 2  $\mu\text{M}$  pyrene in micellar solution of 12-Eg-12 at different [CPC]. (b-d) Plot of  $\ln(I_0/I_q)$  vs [CPC] for all surfactant systems in aqueous solution at 298 K for aggregation number ( $N_{\text{agg}}$ ) measurements.

Aggregation number ( $N_{agg}$ ) of micelle has been estimated by diminishing fluorescence intensity of pyrene with varying the [quencher] (CPC, 0.005 – 0.05 mM) at fixed [pyrene] and [surfactant] (well above their cmcs). Representative plot (of only 12-Eg-12) has been shown in Figure 9a. In the case of immobile and static quencher, I vibration peak of pyrene has been used to obtain the ratio of fluorescence intensities in the absence ( $I_0$ ) and presence ( $I_Q$ ) of quencher (CPC). Then  $I_0 / I_Q$  is plotted against the quencher concentration ([CPC]), resulting a straight line. The  $N_{agg}$  has been calculated from the slopes of such the linear plots (Figure 9b-d). The uncertainty in  $N_{agg}$  was not more than  $\pm 2$ . All  $N_{agg}$  values are listed in Table 4.

**Table 4.** Correlation Coefficient ( $R$ ), Aggregation Number ( $N_{agg}$ ), Stern-Volmer Constant ( $K_{sv}$ ), Micro-Polarity ( $I_1/I_3$ ) and Apparent Dielectric Constant ( $\epsilon_a$ ) of conventional and gemini Surfactants in aqueous solution at 298 K.

Gemini Surfactants	Aggregation Number ( $N_{agg}$ )	Stern Volmer Constant ( $K_{sv} \times 10^4$ )	Micro-polarity ( $I_1/I_3$ )	Apparent Dielectric Constant ( $\epsilon_a$ )
DTAB	148	0.550	1.261	19.98
TTAB	65	1.254	1.240	18.77
CTAB	59 (63) <sup>a</sup>	2.694	1.196	15.27
12-4-12	23	0.972	1.328	25.78
14-4-14	25	0.747	1.297	23.35
16-4-16	15	0.847	1.155	12.00
12-Eda-12	35	1.541	1.228	17.86
14-Eda-14	28	0.868	1.194	15.07
16-Eda-16	21	1.281	1.154	11.92
12-Eg-12	29	1.111	1.237	18.58
14-Eg-14	20	0.597	1.272	21.35
16-Eg-16	13	1.024	1.202	15.75
12-Isb-12	24	0.884	1.315	24.73
14-Isb-14	17	0.473	1.318	25.02
16-Isb-16	21	0.711	1.251	19.66
12-4-12-A	33	1.157	1.061	4.501

<sup>a</sup>data used as such form [55]

The lower value of  $N_{agg}$  for geminis than their conventional counter-parts may be due to chain packing and the nature of hydrophilic / hydrophobic spacer. The presence of more polar atoms in the spacer makes it more hydrophilic (ability of the spacer to associate with more water molecules) than the methylene based spacer. Compared to C-C (1.54 Å), C-O has less bond length (1.36 Å) which bring the head groups nearer despite the electrostatic consequences. Furthermore, hydrophilic spacer based gemini contains  $Cl^-$  as counterion, which is known to bind less (Table 4) than  $Br^-$  to the head groups [19]. Probably, hydrophilicity of the spacer, less bond length and greater  $\alpha$  are responsible for the lower  $N_{agg}$ . However, amide spacer based geminis show higher  $N_{agg}$  in their own class (Table 4). This suggests that, within hydrophilic spacer, packing parameters / micellar arrangement can also influence the  $N_{agg}$ . However, the trend of  $N_{agg}$  decrease with increases in  $m$  is similar to reported in literature (except  $m$ -Isb- $m$ ) [32]. Anionic gemini (12-4-12-A) have found even higher  $N_{agg}$  (more number of monomers in micelle) compared to all cationic geminis. This is in line to surface parameter data (Table 3).

The microenvironment results obtained from fluorescence quenching (from Figure 9b-d) are compiled in Table 4. The micro-polarity of the surfactant micelle can be evaluated by  $I_1/I_3$  (Figure 9a). The higher value of  $I_1/I_3$  reflects a more polar environment. It has been reported that the  $I_1/I_3$  values typically range from 1.8 in water to 0.6 for hydrocarbon solvent [56]. The  $I_1/I_3$  values are well in the range suggesting that the microenvironment felt by pyrene in micellar solution is in between aqueous hydrocarbon (semi-polar). This polarity clearly demonstrates that, in amide spacer based geminis ( $m$ -Eda- $m$ ), pyrene is localized at the end of the palisade layer in the micelle (similar to an n-alkanols with a 3 to 4 carbon chain). However, lowest  $I_1/I_3$  value (1.061) of anionic gemini (12-4-12-A) clearly indicates that pyrene is

localized even more non polar environment (probably deeper inside the palisade layer of the micelle). This may be due to tighter packing of the micelle (Table 3).

Apparent dielectric constant ( $\epsilon_a$ ), of the medium (to solubilize pyrene), was calculated from the relation:  $I_1/I_3 = 1.00461 + 0.01253\epsilon_a$  [19].  $\epsilon_a$  values (Table 4) also support the micro-polarity results.

Stern-Volmer binding constant ( $K_{sv}$ ) (using  $I_0/I_q = 1 + K_{sv} [Q]$ ) is a measure of the hydrophobicity of the environment in which the probe and quencher are located. The  $K_{sv}$  values are obtained from the slope of the plot  $I_0/I_q$  vs  $[Q]$  (Figure 9a-c). The higher value of  $K_{sv}$  denotes the greater solubility of pyrene and CPC. Mostly, conventional surfactants show the hydrophobic environment. However, within geminis, amide spacer based geminis showing the hydrophobic environment for probe and quencher than the other ones.

### 3.3.5. Temperature Effect on Micellization (U-Shaped Behavior)

In surface science, temperature ( $T$ ) plays a crucial role in formation of micelles. Conductivity measurements (among other listed methods) have been used to study the micellization behavior (mainly cmc) of conventional as well as gemini surfactants in aqueous solution at different temperatures (from 283 to 323 K). Figure 10 show representative plots of  $\kappa$  vs [surfactant] (a few surfactants) as a function of temperature. Micellization study of 12-4-12-A has also been performed (over the temperature range) for comparison purposes (Figure 10). Throughout the temperature range, cmc values of all surfactants show dependence on temperature. cmc values are plotted against temperature (Figure 11).

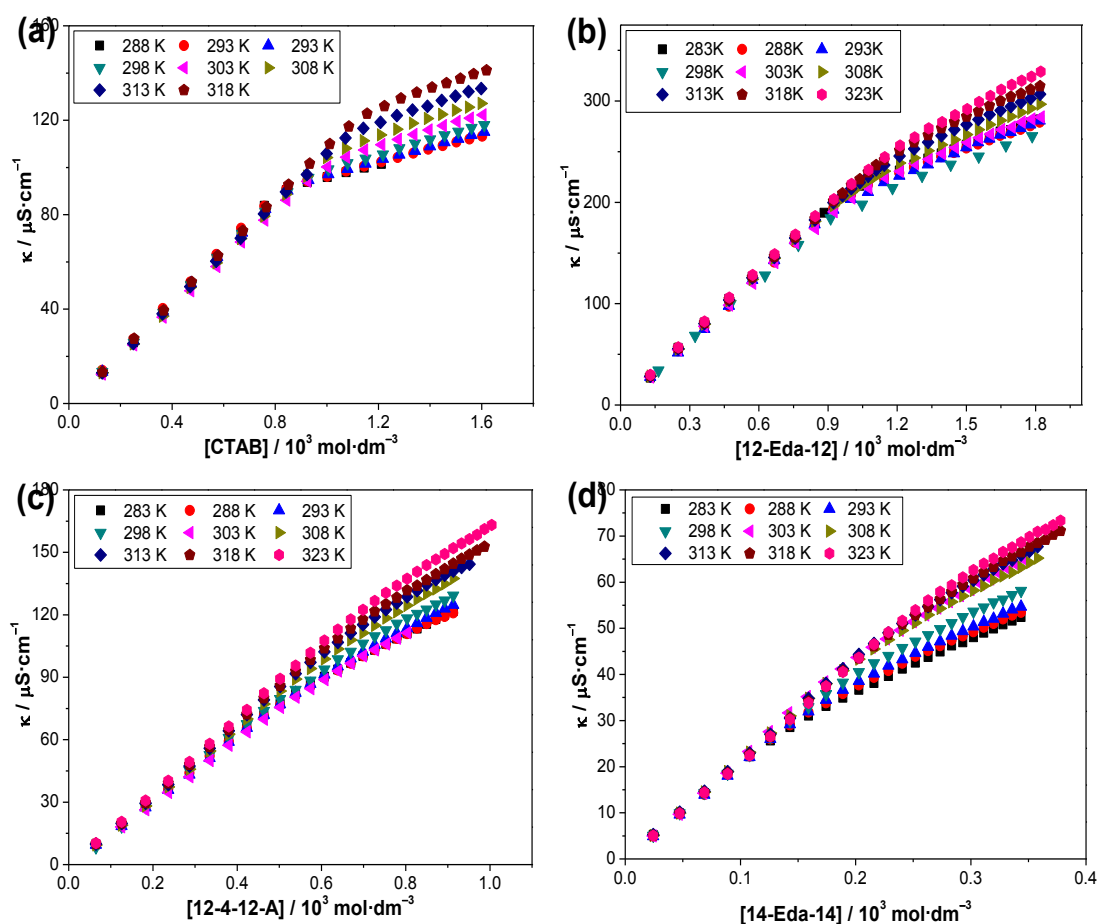


**Figure 10.** Representative plot of specific conductance ( $\kappa$ ) vs [surfactant] at different temperatures (from 283 to 323 K): (a) CTAB; (b) cationic gemini (12-Eda-12); (c) anionic gemini (12-4-12-A); (d) cationic gemini (14-Eda-14).

From Figure 11a-d, it can be seen that cmc decreases up to a certain value ( $cmc_m$ ) and then increases again with continuous increase in the temperature (U-shaped behavior). The initial heating causes the decrease in hydration of the hydrophilic head group which favors micellization. Probably, this may be the reason for the decrease in the cmc up to a certain minimum temperature,  $T_m$  (Figure 11c). When surfactant molecules disperse in the aqueous solution, the alkyl tail group distorts the water structure. Raising the temperature also causes a breakdown of structured water around the alkyl tail part (which opposes the micellization). Above two factors, (i) decrease in head group hydration and (ii) breakdown of structured

water around tail part; compete for the resulting effect on micellization and the cmc value.

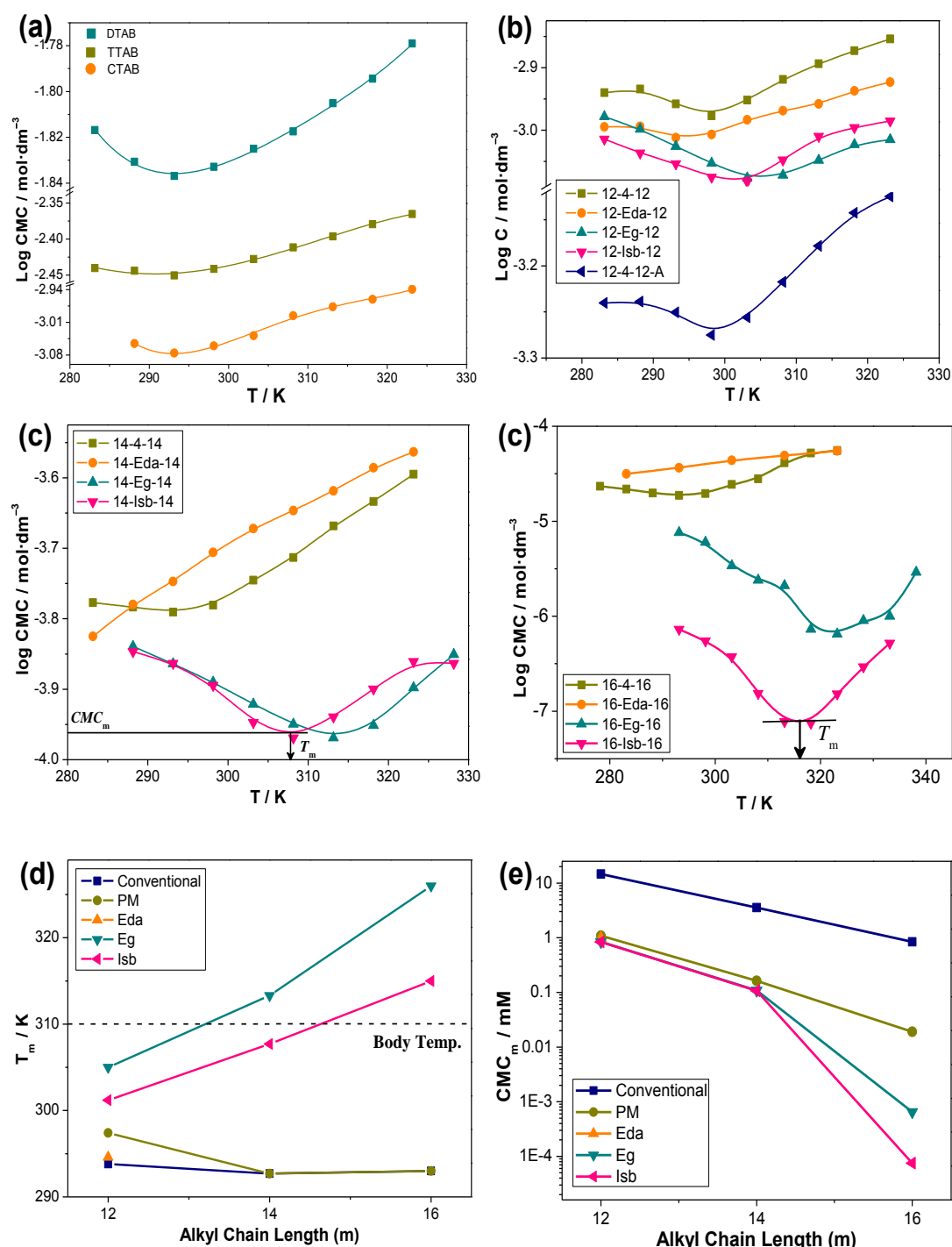


**Figure 11.** Temperature ( $T$ ) dependent U-shaped behavior (Plot of  $\log C$  (logarithm of cmc) vs temperature (K) of: (a) conventional surfactants; (b) 12 series cationic and anionic geminis; (c) 14 series geminis; (d) 16 series geminis in aqueous system. (e) Plot of temperature of minimum cmc ( $T_m$ ) and (f) cmc minimum ( $\text{cmc}_m$ ) vs alkyl chain length ( $m$ ) of all surfactants, respectively.

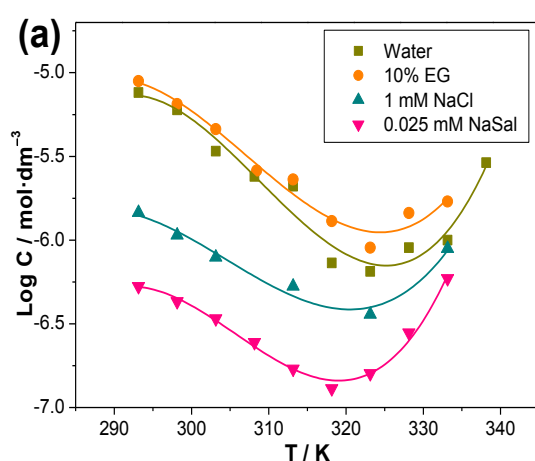
The cmc increase in the latter part of the plot (Figure 11) may be due to the predominance of second factor. However, amide spacer based geminis (*m*-Eda-*m*) show temperature dependent linear behavior with good correlation coefficient (except 12-Eda-12). This mainly happens because of predominance of second effect even at lower temperature. The data strongly suggest that the nature of spacer can influence the micelle formation at a particular temperature. A detailed study of temperature effect on micelle formation of ionic as well as on nonionic conventional surfactants has been reported earlier [8]. However, only a few studies have been reported on U-shaped behavior particularly on cationic geminis [21, 26, 57]. Reported  $T_m$  values of geminis with polymethylene spacer are ~303 K (and between 290-303 K for ionic conventional surfactants [8]. This trend has been followed by conventional and *m*-4-*m* in the present study too (Figure 11e). In addition,  $T_m$  value of 12-4-12-A (298.5 K) has also found similar to *m*-4-*m*. Interestingly,  $T_m$  values of conventional surfactants were found equal to that of *m*-4-*m* and 12-4-12-A, though, it has no spacer and head group effect (Figure 11e). The values of conventional surfactant are also found in good agreement with the earlier report [58] which confirms the validity of the measurements.

It is interesting to note that  $T_m$  values of ester and isosorbide spacer based geminis with  $m = 14$  and 16 are found within 308-326 K (Figure 11e). This range falls well within the range reported for non-ionic surfactants (310-334 K) [8]. This may be due to additional hydration of hydrophilic spacer, which contributes more towards micellar surface. Therefore, structure of the spacer in gemini surfactants plays an important role to decide the micellization behavior and the temperature influence on it. Hydrophilic spacer based cationic geminis could be useful in bio-applications due to its higher  $T_m$  (near to physiological temperature, 310 K).

$T_m$  value is also found dependent on  $m$ . The value of  $T_m$  increases as the  $m$  of ester and isosorbide spacer based geminis increases (quite opposite to the literature data) [8]. This is mainly happen due to higher hydration of the spacer at the interface. However,  $T_m$  values of polymethylene and conventional surfactants show a weak dependence on  $m$ .

### Effect of Additives on U-Shaped Behaviour of 16-Eg-16

Influence of additives (ethylene glycol, NaCl or NaSal) has also been examined on the U-shaped behavior of 16-Eg-16 (due to its unexpected higher  $T_m$  values (like non-ionic surfactant) and lower  $cmc_m$ ). Hence, temperature effect on the micellization of 16-Eg-16 under variety of solvent conditions (aqueous or aqueous + ethylene glycol mixed solvent (mass fraction ( $\phi = 0.11$ )), and in aqueous salt (sodium chloride, NaCl or sodium salicylate, NaSal, mole fractions ( $x$ ) = 0.95 or 0.33, respectively) have also been performed.  $cmc$  values are plotted against temperature (Figure 12a). For various additives, similar behavior (U-shaped) has been observed and can be understood in the light of factors mentioned in earlier section (3.3.4.).



(b) Table 5.  $T_m$  and  $cmc_m$  of 16-Eg-16 with different fixed [additives].

16-Eg-16 (Gemini)	$T_m$ K	$cmc_m \cdot 10^6$ mol·dm <sup>-3</sup>
Pure water	$326.0 \pm 0.7$	$0.65 \pm 0.03$
$\phi_{EG} = 0.11$	$325.0 \pm 0.5$	$0.90 \pm 0.05$
$x_{NaCl} = 0.95$	$321.0 \pm 0.4$	$0.36 \pm 0.02$
$x_{NaSal} = 0.33$	$318.5 \pm 0.5$	$0.13 \pm 0.01$

Figure 12. (a) Fixed [additive] (ethylene glycol, EG; sodium chloride, NaCl; sodium salicylate, Nasal) effect on U-shaped behavior of ester based gemini with  $m = 16$  (16-Eg-16); (b) Table 5.

From the plot of  $\log C$  vs  $T$  (Figure 12a),  $cmc_m$  and  $T_m$  have been obtained and compiled in Table 5. Addition of a polar organic solvent to water is expected to change the physical properties (dielectric constant ( $\epsilon$ ), dipole moment) [59]. Presence of EG in the solvent mixture can decrease the  $\epsilon$  value ( $\epsilon_{\text{water}} = 78.5$  and  $\epsilon_{\text{EG}} = 37.7$  at 293 K). An overall cmc increase was observed in 0.11  $\phi_{\text{EG}}$  (at different temperature) without affecting  $T_m$  much. The addition of polar organic solvents may decrease the hydrophobic interaction between alkyl groups of the surfactant (diminishing of second factor). Additionally, when  $\epsilon$  decreases the repulsion between the head groups increases and thus cmc value increases (Table 5).

Presence of salt (NaCl or NaSal) in aqueous solution, at a given temperature, causes a decrease in cmc (Figure 12). It may be due to screening of the repulsion between cationic head groups of the surfactant in the presence of counter ions ( $\text{Cl}^-$  or  $\text{Sal}^-$ ) which facilitate early formation of the micelles. This indeed was observed in the present study and confirms the earlier reports [13, 60]. However, a distinct fall in  $T_m$  values was observed in the presence of salts (Table 5). The decrease was more pronounced with the salt containing hydrophobic counter-ion ( $\text{Sal}^-$ ). It has been reported earlier that hydrophobicity of the counter-ion plays an important role in the aggregation process [61].  $\text{Sal}^-$  is known for a stronger binding with the cationic head group and for screening the repulsive coulombic interactions. The presence of salt and increase of temperature may cause decrease in hydration of the hydrophilic group synergistically and, therefore, first factor predominates at lower temperature [8]. However, in presence of salt above factor influences only up to a lower temperature because hydration is partially taken care by counter-ion binding. Beyond this, break down of the structure of water around the alkyl tail (*vide supra*) starts predominating the micellization process and responsible for the lower  $T_m$ .

### 3.3.6. Thermodynamics of Micellization

As it has been stated earlier, micellization of aqueous surfactant solution is responsive to temperature; thermodynamic parameters of all cationic and anionic surfactants have been calculated by temperature dependence of the micellization parameters (Figure 11). For the ionic surfactants, the mass-action model approach is usually preferred. For cationic gemini surfactants, the standard Gibbs free energy of micelle formation per mole of monomer,  $\Delta G_{mic}^{\circ}$ , can be written as [53],

$$\Delta G_{mic}^{\circ} = 2RT (1.5 - \alpha) \ln X_{cmc} \quad (6)$$

Where,  $R$ ,  $T$  and  $X_{cmc}$  are ideal gas constant, absolute temperature and cmc expressed in mole fraction unit, respectively.

The standard enthalpy changes for micellization,  $\Delta H_{mic}^{\circ}$ , can be calculated by using Gibbs-Helmholtz equation,

$$\Delta H_{mic}^{\circ} = -2RT^2 (1.5 - \alpha) \left( \frac{\partial \ln X_{cmc}}{\partial T} \right)_P \quad (7)$$

Since,  $\Delta H_{mic}^{\circ}$  is not constant with respect to temperature, therefore, the values of  $(\partial(\ln X_{cmc}) / \partial T)_P$  were obtained by using third order of polynomial equation (Eq. 8) for all systems except 14-eda-14 and 16-eda-16 [62]. For these geminis, a linear correlation was obtained and the value of the slope was directly taken as the value of  $\partial(\ln X_{cmc}) / \partial T$ .

$$\ln X_{cmc} = a + bT + cT^2 + dT^3 \quad (8)$$

On differentiating Eq. 8, one can get the value of  $\partial \ln X_{cmc} / \partial T$  as,

$$\frac{\partial \ln X_{cmc}}{\partial T} = b + 2cT + 3dT^2 \quad (9)$$

The polynomial constants ( $a$ ,  $b$ ,  $c$  and  $d$ ) are obtained by least square regression analyses. By substituting the value  $\partial \ln X_{cmc} / \partial T$  in to Eq. 7, one can

$$\Delta H_{mic}^{\circ} = -2RT^2 (1.5 - \alpha) (b + 2cT + 3dT^2) \quad (8)$$

Finally, the standard entropy of the micellization,  $\Delta S_{mic}^{\circ}$ , is evaluated from the values of  $\Delta H_{mic}^{\circ}$  and  $\Delta G_{mic}^{\circ}$  as follows,

$$\Delta S_{mic}^{\circ} = \frac{(\Delta H_{mic}^{\circ} - \Delta G_{mic}^{\circ})}{T} \quad (9)$$

The calculated thermodynamic parameters ( $\Delta G_{mic}^{\circ}$ ,  $\Delta H_{mic}^{\circ}$  and  $\Delta S_{mic}^{\circ}$ ) for all surfactant systems are listed in Table 6 and 7. Negative value of  $\Delta G_{mic}^{\circ}$  tells spontaneous micelle formation in aqueous solution for all surfactant systems. However,  $\Delta G_{mic}^{\circ}$  follows the order:  $m-4-m > m-Eda-m > m-Eg-m > m-Isb-m$ , suggesting the nature of spacer dependence. Values of  $\Delta H_{mic}^{\circ}$  are found both positive

( $\Delta H^{\circ}_{\text{mic}} > 0$ , endothermic) and negative ( $\Delta H^{\circ}_{\text{mic}} < 0$ , exothermic) for different to different surfactants studied (at large temperature range), suggesting the dependency of the phenomenon on nature of the spacer. As reported earlier by Zana [63], enthalpy of micellization governed by several factors: (a) release of water molecules surrounded to hydrophobic tail; (b) electrostatic interaction between head groups (repulsive), between counter-ions (repulsive) and between head group and counter-ion (attractive). The first factor is mainly responsible for the negative value of  $\Delta H^{\circ}_{\text{mic}}$ . The more negative values of  $\Delta H^{\circ}_{\text{mic}}$ , for CTAB and *m*-Isb-*m*, indicate about release of even more water molecule surrounding the alkyl tail, resulting in to more hydrophobic interactions. This favors the micellization and lead to a more compact micelle in solution [63, 64]. Above finding (more negative  $\Delta H^{\circ}_{\text{mic}}$  with the isosorbide spacer based geminis) clearly suggests that *m*-Isb-*m* (chiral center), two alkyl chains, remain in *cis* confirmations after aggregate formed. However, they may be switchable between *trans* and *cis* before cmc [65].

Interestingly, with 16-*s*-16, micellization process is entropy driven up to  $T_m$  and then slowly converts to enthalpy driven process (at higher temperature) except 16-Eda-16. The value of negative enthalpy indicates that the London dispersion forces have a significant role in the micellization process at higher temperatures [66]. These forces are of predominant nature and decide micellization at higher temperatures. Moreover, values of  $\Delta S^{\circ}_{\text{mic}}$  (Table 6 and 7) decrease with increase in hydrophilicity of the spacer, indicating the reduction in randomness of the system.  $\Delta S^{\circ}_{\text{mic}}$  is also responsible for the negative value of  $\Delta G^{\circ}_{\text{mic}}$ . Here,  $\Delta H^{\circ}_{\text{mic}}$  is much smaller than the  $T\Delta S^{\circ}_{\text{mic}}$  in all cases suggesting that the micellization is entropy driven process. However, above trend is not followed for anionic gemini surfactant (12-4-12-A). This may be due to the different structure of the head group present in 12-4-12-A.

**Table 6.** Thermodynamic parameters ( $\Delta G^{\circ}_{\text{mic}}$ ,  $\Delta H^{\circ}_{\text{mic}}$  and  $\Delta S^{\circ}_{\text{mic}}$ ) of conventional and cationic and anionic gemini surfactants (12 series) in aqueous solution at different temperatures ( $T$ ).

$T$ K	$\Delta G^{\circ}_{\text{mic}}$ kJ·mol <sup>-1</sup>	$\Delta H^{\circ}_{\text{mic}}$ kJ·mol <sup>-1</sup>	$\Delta S^{\circ}_{\text{mic}}$ kJ·K <sup>-1</sup> ·mol <sup>-1</sup>	$T$ K	$\Delta G^{\circ}_{\text{mic}}$ kJ·mol <sup>-1</sup>	$\Delta H^{\circ}_{\text{mic}}$ kJ·mol <sup>-1</sup>	$\Delta S^{\circ}_{\text{mic}}$ kJ·K <sup>-1</sup> ·mol <sup>-1</sup>
<b>DTAB</b>				<b>12-4-12</b>			
283	-68.03	-41.85	0.092	283	-63.96	161.64	0.797
288	-68.77	-41.46	0.095	288	-64.10	159.28	0.775
293	-69.63	-41.22	0.097	293	-65.75	159.64	0.769
298	-70.38	-41.03	0.098	298	-65.77	156.20	0.744
303	-70.49	-40.52	0.099	303	-67.01	157.17	0.739
308	-70.61	-40.02	0.099	308	-65.17	151.27	0.702
313	-70.96	-39.72	0.100	313	-65.91	151.19	0.693
318	-70.27	-38.84	0.099	318	-67.00	151.84	0.688
323	-69.36	-37.92	0.097	323	-63.96	143.21	0.641
<b>TTAB</b>				<b>12-Eda-12</b>			
283	-80.94	8.30	0.315	283	-56.89	15.32	0.255
288	-82.10	8.22	0.313	288	-58.29	15.41	0.256
293	-82.90	8.13	0.311	293	-57.61	14.90	0.247
298	-83.23	8.02	0.306	298	-59.72	15.18	0.251
303	-82.48	7.82	0.298	303	-58.27	14.63	0.240
308	-84.72	7.92	0.301	308	-57.41	14.21	0.232
313	-83.28	7.69	0.291	313	-58.17	14.20	0.231
318	-83.53	7.63	0.287	318	-57.68	13.93	0.225
323	-83.36	7.55	0.281	323	-54.45	13.00	0.209
<b>CTAB</b>				<b>12-Eg-12</b>			
288	-34.85	-257.62	-0.77	283	-36.09	123.28	0.563
293	-35.62	-255.68	-0.75	288	-33.91	113.54	0.512
298	-35.68	-253.45	-0.73	293	-31.48	103.12	0.459
303	-35.45	-249.71	-0.71	298	-33.43	107.19	0.472
308	-34.92	-248.84	-0.69	303	-40.49	127.19	0.553
313	-34.82	-244.45	-0.67	308	-29.88	92.52	0.397
318	-34.74	-241.52	-0.65	313	-31.82	97.54	0.413
323	-35.02	-243.41	-0.64	318	-34.35	104.35	0.436
<b>12-4-12-A</b>				323	-38.64	115.96	0.478
283	-44.63	172.46	0.217	<b>12-Isb-12</b>			
288	-46.02	174.83	0.221	283	-30.72	-401.13	-1.308
293	-44.85	167.09	0.212	288	-32.95	-439.72	-1.412
298	-45.84	164.14	0.210	293	-32.38	-441.80	-1.397
303	-42.37	152.43	0.195	298	-33.78	-470.50	-1.465
308	-45.65	162.77	0.208	303	-38.97	-555.19	-1.703
313	-48.64	172.03	0.221	308	-34.58	-508.09	-1.537
318	-48.49	170.06	0.219	313	-35.28	-534.49	-1.594
323	-47.10	163.32	0.210	318	-35.00	-543.91	-1.600
				323	-35.49	-564.67	-1.638

**Table 7.** Thermodynamic parameters ( $\Delta G^{\circ}_{\text{mic}}$ ,  $\Delta H^{\circ}_{\text{mic}}$  and  $\Delta S^{\circ}_{\text{mic}}$ ) of cationic gemini surfactants (14 and 16 series) in aqueous solution at different temperatures ( $T$ ).

$T$ K	$\Delta G^{\circ}_{\text{mic}}$ kJ·mol <sup>-1</sup>	$\Delta H^{\circ}_{\text{mic}}$ kJ·mol <sup>-1</sup>	$\Delta S^{\circ}_{\text{mic}}$ kJ·K <sup>-1</sup> ·mol <sup>-1</sup>	$T$ K	$\Delta G^{\circ}_{\text{mic}}$ kJ·mol <sup>-1</sup>	$\Delta H^{\circ}_{\text{mic}}$ kJ·mol <sup>-1</sup>	$\Delta S^{\circ}_{\text{mic}}$ kJ·K <sup>-1</sup> ·mol <sup>-1</sup>
<b>14-4-14</b>				<b>16-4-16</b>			
283	-70.01	39.34	0.386	278	-55.01	052.34	0.386
288	-70.36	38.78	0.379	283	-53.48	024.53	0.276
293	-73.35	39.65	0.385	288	-50.51	001.50	0.181
298	-65.28	34.73	0.335	293	-55.94	-018.57	0.128
303	-67.12	35.32	0.338	298	-59.66	-037.50	0.074
308	-70.55	36.71	0.348	303	-61.98	-053.66	0.027
313	-66.65	34.40	0.323	308	-53.50	-054.95	-0.005
318	-66.64	34.08	0.317	313	-64.68	-073.03	-0.027
323	-66.54	33.78	0.310	318	-63.13	-071.65	-0.027
<b>14-Eda-14</b>				<b>16-Eda-16</b>			
283	-55.83	-18.42	0.132	283	-62.48	-17.34	0.159
288	-57.24	-19.37	0.131	293	-64.19	-18.64	0.155
293	-57.18	-19.80	0.128	303	-59.65	-18.14	0.137
298	-55.69	-19.77	0.121	313	-67.63	-21.43	0.148
303	-56.11	-20.38	0.118	323	-55.42	-18.27	0.115
308	-57.39	-21.29	0.117	<b>16-Eg-16</b>			
313	-56.21	-21.30	0.112	293	-57.03	011.65	0.234
318	-55.09	-21.33	0.106	298	-62.03	073.45	0.454
323	-55.40	-21.89	0.104	303	-53.58	094.15	0.487
<b>14-Eg-14</b>				<b>16-Isb-16</b>			
288	-47.91	70.25	0.410	293	-085.81	142.04	0.777
293	-47.10	67.93	0.391	298	-079.95	152.67	0.780
298	-45.44	63.87	0.367	303	-100.53	187.20	0.949
303	-45.26	62.22	0.355	308	-108.03	160.61	0.872
308	-46.97	63.18	0.357	313	-123.12	106.93	0.735
313	-49.08	64.71	0.363	318	-116.69	-000.06	0.367
318	-49.07	63.83	0.355	323	-090.05	-110.15	-0.062
323	-54.18	70.00	0.384	328	-077.99	-224.61	-0.447
328	-51.26	65.73	0.357	333	-074.76	-374.42	-0.899
<b>14-Isb-14</b>							
288	-52.58	-82.39	-0.103				
293	-43.41	-66.50	-0.079				
298	-50.51	-75.53	-0.084				
303	-48.18	-70.14	-0.072				
308	-45.00	-64.17	-0.062				
313	-53.23	-75.05	-0.070				
318	-47.98	-66.98	-0.060				
323	-55.68	-76.91	-0.066				
328	-49.07	-66.47	-0.053				

### Enthalpy-Entropy Compensation

In general, the compensation phenomenon between the  $\Delta H_{mic}^{\circ}$  and  $\Delta S_{mic}^{\circ}$  for the micellization process can be described (Figure 13) in the form of a straight line equation of the type,

$$\Delta H_{mic}^{\circ} = T_C \Delta S_{mic}^{\circ} + \Delta H_{mic}^{*} \quad (10)$$

The slope of the straight line represents compensation temperature ( $T_C$ ) and is a characteristic of solute-solute and solute-solvent interactions.  $T_C$  can be considered as a measure of “desolvation” part of the micellization phenomenon (dehydration of the hydrocarbon tail). The intercept,  $\Delta H_{mic}^{*}$ , characterize the solvent-solvent interaction and can be considered as an index of the chemical part of the micellization (aggregation of hydrocarbon tails into the micelle).

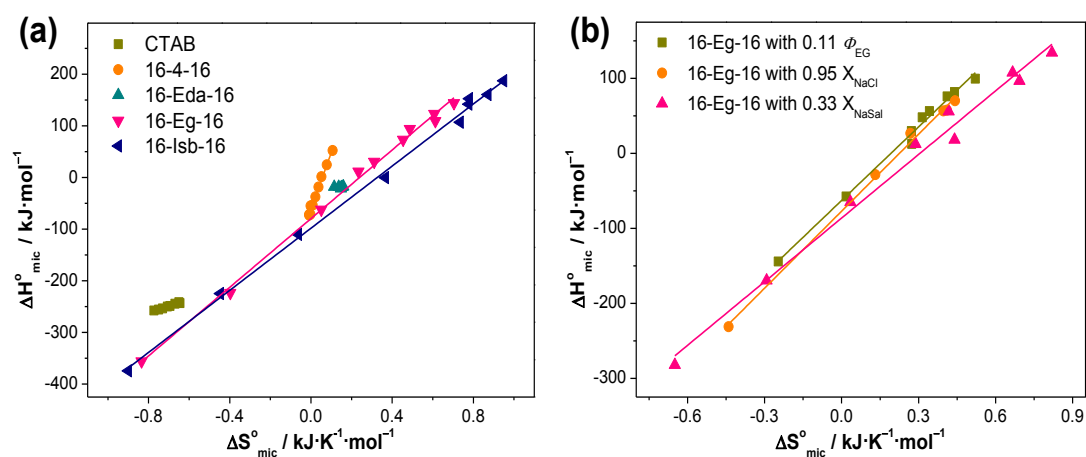


**Figure 13.** Plot of standard enthalpy ( $\Delta H_{mic}^{\circ}$ ) vs standard entropy ( $\Delta S_{mic}^{\circ}$ ) for, (a) 16 series cationic gemini and conventional surfactants; (d) 16-Eg-16 with additives, in aqueous solution at 298 K.

Unfortunately, enthalpy- entropy compensation behavior is not studied much in case of gemini surfactants. Also, the present case, the satisfactory data could be

obtained with a few gemini surfactants only (16-Eg-16, 16-Isb-16 or 14-Isb-14). The  $T_c$  values are 332, 301 and 293 K, respectively, which is in the range reported for conventional surfactants [8]. However,  $T_c$  values could not be obtained (or out of range) for other geminis and left out from the discussion.

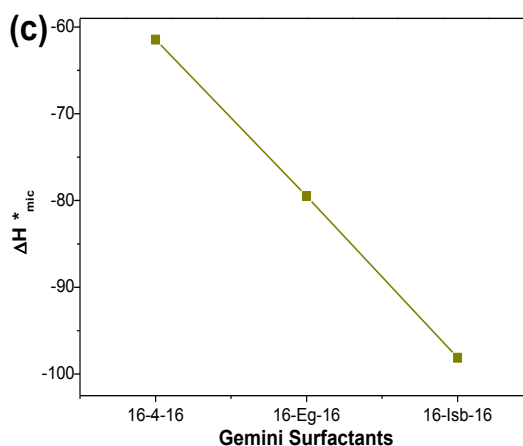


**Figure 14.** Variation of  $\Delta H^*_{mic}$  with nature of the spacer.

It is intriguing to note that  $\Delta H^*_{mic}$  decreases linearly with changing the nature of the spacer in 16-s-16 series (Figure 14). The decrease in  $\Delta H^*_{mic}$  corresponds to increase in the stability of the micelle and lower cmc. Therefore, more stable micelles are formed with *Isb*-spacer. This may be due to increased hydrophilic nature of the 16-Isb-16 monomer which contributes in the phenomenon of stable micellization. This indeed has been reflected from relatively lower cmc values of 16-Isb-16 in the temperature range studied (Figure 11d).

### 3.3.7. Monomer Arrangement and Size of the Micelle

Micellar size and shape of geminis are directly / indirectly influenced by micro-polarity and thermodynamic parameters. Therefore, it is of genuine interest to understand the micellar size / shape and molecular interactions present in the solution.

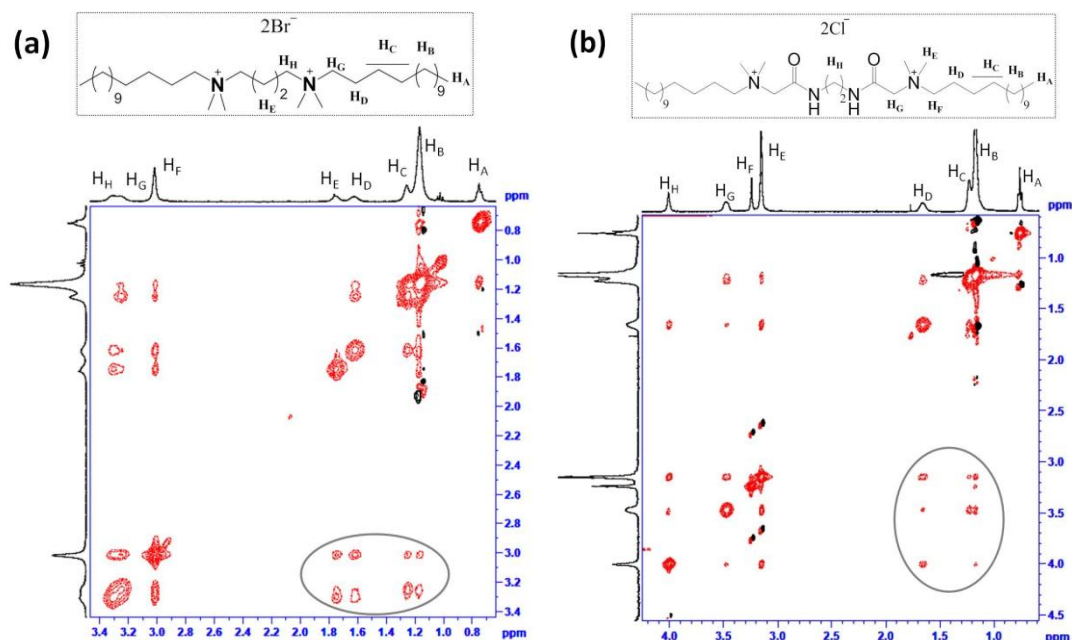
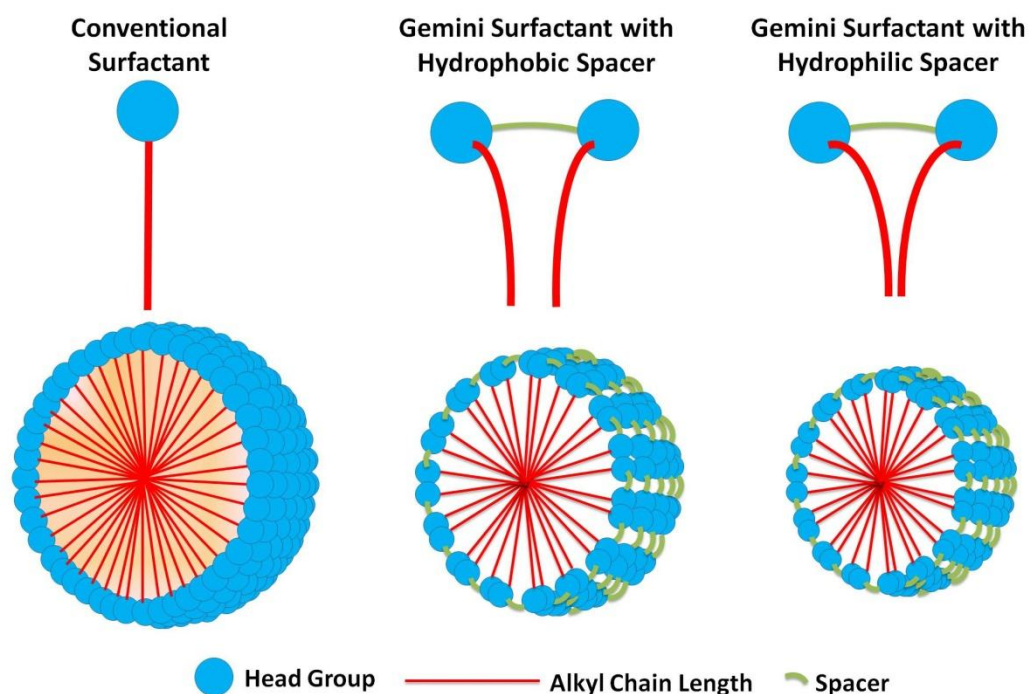


**Figure 15.** 2D NOESY  $^1\text{H}$  NMR spectra of gemini surfactants (well above their cmc  $\sim 1.5$  mM) with their chemical structure and annotation in  $\text{D}_2\text{O}$  at 298 K: (a) 14-4-14; (b) 14-Eda-14.

2D NOESY  $^1\text{H}$  NMR measurements are performed for 14-4-14 and 14-Eda-14 above their cmc values (1.5 mM, Figure 15). Intermolecular (cross-peaks) NOESY interactions between spacer and alkyl chain have been observed (Figure 15). There are mainly strong cross-peaks between  $\text{H}_\text{H} - \text{H}_\text{D}$  and  $\text{H}_\text{C} - \text{H}_\text{H}$  protons of 14-4-14 (Figure 15a), indicating that 2<sup>nd</sup> or 3<sup>rd</sup> carbon protons near the head group ( $-\text{N}^+(\text{CH}_3)_2$ ) are close enough to  $\alpha$  or  $\beta$  carbon protons of the spacer. However, in case of 14-Eda-14 (Figure 15b), such cross-peaks of protons like  $\text{H}_\text{B} - \text{H}_\text{F}$  and  $\text{H}_\text{B} - \text{H}_\text{H}$  are also present, suggesting that the 4-5<sup>th</sup> carbon protons of the alkyl tail are close enough to the center ethylene protons ( $\text{H}_\text{H}$ ) of the spacer.

Above observations clearly suggest that the hydrophilic spacer based gemini may give smaller and compact micellar structure than the polymethylene spacer based gemini (14-4-14) (Scheme 2). Similar thoughts are presented by Wang et al in recent review article [67]. From earlier reports [53], it has already been noticed that

hydrophilic spacer and hydrophobic spacer ( $\sim C < 10$ ) remain horizontal to the surface (from earlier section 3.3.3.). So, alkyl chain with certain carbon number can bend toward the spacer protons. Due to above reason, hydrophilic spacer based geminis have compact micellar structure.



**Scheme 2.** Schematic representation of monomeric arrangement in to micellar structure for conventional and gemini surfactants.

DLS measurements are also performed to analyze actual micellar size of conventional and gemini surfactant micelle (Figure 16) to prove above propositions based on 2D NOESY measurements.

DLS data show that the hydrodynamic diameter ( $D_h$ ) of 12 series and 14 series gemini and conventional surfactants, varies in the range of 1.3 – 3.2 nm (reflecting the typical size of a spherical aggregates). However, the micellar size of DTAB and TTAB are higher than the gemini surfactants. This is mainly due to more number of monomers in the micellar structure of conventional surfactant (see earlier section).

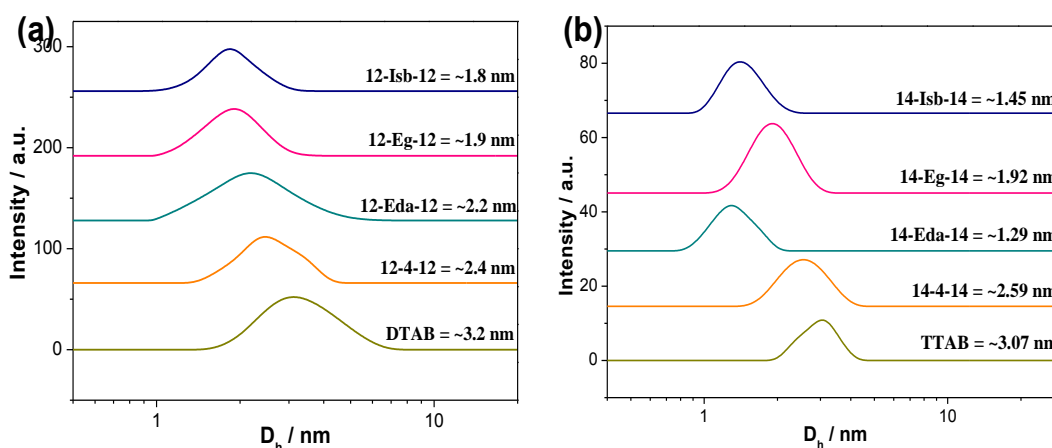


**Figure 16.** Micelle size (hydrodynamic diameter,  $D_h$ ) of surfactants above their CMC: (a) 12 series conventional (DTAB, 30 mM) and gemini surfactants (2.5 mM); (b) 14 series conventional (TTAB, 10 mM) and geminis (1.5 mM).

Interestingly, the micellar size of polymethylene based geminis (12-4-12 and 14-4-14) are higher than the hydrophilic spacer based geminis. The results of micellar arrangement and size of geminis were well matched by both the techniques (2D NOESY and DLS), suggesting that hydrophilic spacer based gemini produces compact micelle with smaller size than conventional / hydrophobic spacer based geminis (See Scheme 2).

### 3.4. Conclusion

Solution behaviors, of biocompatible spacer based cationic gemini surfactants, have been studied. Data related to various micellar phenomenon (solubilization, cmc, surface parameters, micropolarity and micellar size / arrangements) are collected and compared with polymethylene spacer based gemini and conventional cationic surfactants. Based on the results following conclusions are drawn:

- By all techniques (conductivity, tensiometry, fluorescence and  $^1\text{H}$  NMR) result similar values of cmc. Biocompatible (in particular ester or isosorbide) spacer based geminis show lower cmc, higher  $\alpha$  and lower  $T_k$  compared to other geminis.
- Ester and isosorbide spacer based gemini surfactants have better surface properties (higher packing density at air-water interface) among others. However, 12-4-12-A (anionic gemini) have shown tighter packing density compared to the other surfactants.
- From the micro-polarity results, it can be seen that the pyrene is localized at the end of the palisade layer of micelle of cationic geminis as well as conventional ones. In case of 12-4-12-A, pyrene has been solubilized even deeper. Among geminis, amide spacer based geminis have higher aggregation number ( $N_{\text{agg}}$ ) and produce more hydrophobic environment than others.
- Novel U-shaped behavior has been observed for all the surfactants except 14-Eda-14 and 16-Eda-16. Temperature minimum ( $T_m$ ) of polymethylene spacer based cationic and anionic geminis and conventional surfactants varies within 290-300 K, indicating no spacer effect. However,  $T_m$  of ester and isosorbide spacer based geminis are found near to physiological temperature. This

information can be use in possible medicinal applications. Thermodynamic parameters show spontaneous micelle formation as well as the process is mainly entropy driven.

- 2D NOESY  $^1\text{H}$  NMR spectra clearly show the bending of hydrophobic chain towards the spacer (more with biocompatible spacer based than polymethylene ones). This resulted into compact micellar structure which is confirmed even by DLS results.

## References

- [1] H. J. Kim, T. Kim, M. Lee, *Acc. Chem. Res.* 44 (2011) 72.
- [2] Kabir-ud-Din, U. S. Siddiqui, S. Kumar, A. A. Dar, *Colloid Polym. Sci.* 284 (2006) 807.
- [3] S. Kumar, N. Parveen, Kabir-ud-Din, *J. Phys Chem. B* 108 (2004) 9588.
- [4] D. Mitra, I. Chakraborty, S. C. Bhattacharya, S. P. Moulik, *Langmuir* 23 (2007) 3049.
- [5] Kabir-ud-Din, P. A. Koya, *J. Chem. Eng. Data* 55 (2010) 1921.
- [6] (a) Kabir-ud-Din, S. Kumar, Kirti, P. S. Goyal, *Langmuir* 12 (1996) 1490; (b) S. L. David, S. Kumar, Kabir-ud-Din, *J. Chem. Eng. Data* 42 (1997) 198; (c) Kabir-ud-Din, D. Bansal, S. Kumar, *Langmuir* 13 (1997) 5071; (d) R. T. Buwalda, M. C. A. Stuart, J. B. F. N. Engberts, *Langmuir* 16 (2000) 6780; (e) P. A. Hassan, S. N. Sawant, N. C. Bagkar, J. V. Yakhmi, *Langmuir* 20 (2004) 4874; (f) G. Garg, P. A. Hassan, V. K. Aswal, S. K. Kulshreshtha, *J Phys Chem B* 109 (2005)1340; (g) U. S. Siddiqui, G. Ghosh, Kabir-ud-Din, *Langmuir* 22 (2006) 9874 and references there in.
- [7] S Kumar, D Bansal, Kabir-ud-Din, *Langmuir* 15 (1999) 4960.
- [8] L-J. Chen, S-Y. Lin, C-C. Huang, *J. Phys. Chem. B* 102 (1998) 4350.
- [9] C. La Mesa, *J. Phys. Chem.* 94 (1990) 323.
- [10] A. Gonzalez-Perez, J. L. Del Castillo, J. Czapkiewicz, J. R. Rodriguez, *J. Phys. Chem. B* 105 (2001) 1720.
- [11] T-M. Perger, M. Bester-Rogac, *J. Colloid Interface Sci.* 313 (2007) 288.
- [12] A. B. Pahi, D. Varga, Z. Kiraly, A. Mastalir, *Colloids Surf. A* 319 (2008) 77.
- [13] B. Sarac, M. Bester-Rogac, *J. Colloid Interface Sci.* 338 (2009) 216.
- [14] G. Bai, J. Wang, H. Yan, Z. Li, R. K. Thomas, *J. Phys. Chem. B* 105 (2001) 3105.
- [15] Z. Y. Zhaoxi, Z. Ou, Y. Yi, Q. Yu, *Acta Chim. Sinica* 59 (2001) 690.
- [16] M. S. Bakshi, A. Kaura, R. K. Mahajan, *Colloids Surf. A* 262 (2005) 168.
- [17] A. B. Pahi, Z. Kitaly, A. Mastalir, J. Dudas, S. Puskas, A. Vago, *J. Phys. Chem. B* 112 (2008) 15320.
- [18] Kabir-ud-Din, P. A. Koya, Z. A. Khan, *J. Colloid Interface Sci.* 342 (2010) 340.
- [19] Kabir-ud-Din, P. A. Koya, *Langmuir* 26 (2010) 7905.
- [20] Kabir-ud-Din, P. A. Koya, Z. A. Khan, *J. Disp. Sci. Tech.* 32 (2011) 558.
- [21] Z. Yan, Y. Li, X. Wang, J. Dan, J. Wang, *J. Mol. Liquids* 161 (2011) 49.
- [22] G. Liu, D. Gu, H. Liu, W. Ding, Z. Li, *J. Colloid Interface Sci.* 358 (2011) 521.
- [23] S. Chavda, K. Kuperkar, P. Bhadur, *J. Chem. Eng. Data* 56 (2011) 2647.
- [24] R. Zarganian, A. K. Bordbar, R. Amiri, M. Tamannaie, A. R. Khosropour, I. Mohammdapoor-Baltork, *J. Soln. Chem.* 40 (2011) 921.
- [25] C. Batigoc, H. Akbas, M. Boz, *J. Chem. Thermodynamics* 43 (2011) 1349.
- [26] M. H. Alimohammadi, S. Javadian, H. Gharibi, A. R. Tehrani-Bhagha, M. R. Alavijeh, K. Kakaei, *J. Chem. Thermodynamics* 44 (2012) 107.
- [27] S. D. Wetting, X. Li, R. E. Verral, *Langmuir* 19 (2003) 3666.

- [28] G. Bai, H. Yan, R. K. Thomas, *Langmuir* 17 (2001) 4501.
- [29] R. Zana, *J. Colloid Interface Sci.* 252 (2002) 259.
- [30] M. Tachiya, *Chem. Phys. Lett.* 33 (1975) 289.
- [31] N.J. Turro, A. Yekta, *J. Am. Chem. Soc.* 100 (1978) 5951.
- [32] R. Zana, J. Xia, Gemini Surfactants: Synthesis, Interfacial, Solution Phase Behavior, Application, Marcel Dekker, New York, 2004.
- [33] M. Rose, R. Palkovits, *Chem. Sus. Chem.* 5 (2012) 167.
- [34] (a) A. Domingez, A. Fernandez, N. Gonzalez, E. Iglesias, L. Montenegro, *J. Chem. Education* 74 (1997) 1227; (b) E. Fuguet, C. Rafols, M. Roses, E. Bosch, *Anal. Chem. Acta* 548 (2005) 95; (c) T. Asakawa, Y. Shimizu, T. Ozawa, A. Ohta, S. Miyagishi, *J. Oleo Sci.* 57 (2008) 243 and reference there in.
- [35] (a) B. Sohrabi, A. Bazyari, M. Hashemianzadeh, *Colloids and Surfaces A* 364 (2010) 87; (b) M. D. M. Graciani, M. Munoz, A. Rodriguez, M. L. Moya, *Langmuir* 21 (2005) 3303.
- [36] L. M. Zhou, X. H. Jiang, Y. T. Li, Z. Chen, X. Q. Hu, *Langmuir* 23 (2007) 11404.
- [37] Q. Zhang, Z. Gao, F. Xu, S. Tai, X. Liu, S. Mo, F. Niu, *Langmuir* 28 (2012) 11979.
- [38] X. Huang, Y. Han, Y. Wang, M. Cao, Y. Wang, *Colloids Surf. A* 325 (2008) 26 and reference there in.
- [39] (a) W. Guo, B. M. Fung, S. D. Christian, *Langmuir* 8 (1992) 446; (b) N. D. Gillitt, G. Savelli, C. A. Bunton, *Langmuir* 22 (2006) 5570; (c) J-H. Lin, W-S. Chen, S-S. Hou, *J. Phys. Chem. B* 117 (2013) 12076.
- [40] (a) X. Huang, Y. Han, Y. Wang, Y. Wang, *J. Phys. Chem. B* 111 (2007) 12439; (b) Y. Jiang, H. Chen, X-H. Cui, S-Z. Mao, M-L. Liu, P-Y. Luo, Y-R. Du, *Langmuir* 24 (2004) 3118; (c) X. Zhang, X. Peng, L. Ge, L. Yu, Z. Liu, R. Guo, *Colloid Polym. Sci.* 292 (2014) 1111.
- [41] (a) T. Singh, A. Kumar, *J. Phys. Chem. B* 111 (2007) 7843.
- [42] (a) B-O. Persson, T. Drakenberg, B. Lindman, *J. Phys. Chem.* 80 (1976) 2124; (b) T. W. Davey, W. A. Ducker, A. R. Hayman, *Langmuir* 16 (2000) 2430.
- [43] E. B. Tada, L. P. Novaki, O. A. El Seoud, *Langmuir* 17 (2001) 652.
- [44] B-O. Persson, T. Drakenberg, B. Lindman, *J. Phys. Chem.* 83 (1979) 3011.
- [45] C. M. C. Faustino, A. R. T. Calado, L. Garcia-Rio, *J. Colloid and Interface Sci.* 351 (2010) 472.
- [46] S. De, V. K. Aswal, P. K. Goyal, S. Bhattacharya, *J. Phys. Chem.* 100 (1996) 11664.
- [47] G. Zhinong, T. Shuxin, Z. Qi, Z. Yu, L. Bo, G. Yushu, H. Li, T. Xiaoyan, *Wuhan Univ. J. Nat. Sci.* 13 (2008) 227.
- [48] X. Wang, J. Wang, Y. Wang, H. Yan, *Langmuir* 20 (2004) 53
- [49] P. A. Koya, Kabir-ud-din, *J. Colloid Interface Sci.* 360 (2011) 175.
- [50] D-Y. Zhu, F. Cheng, Y. Chen and S-C. Jiang, *Colloid Surf. A* 397 (2012) 1.
- [51] (a) A. Bhadani, H. Kataria, S. Singh, *J. Colloid Interface Sci.* 361 (2011) 33; (b) A. Bhadani, S. Singh, *Langmuir* 27 (2011) 14033.
- [52] L. D. Song, M. J. Rosen, *Langmuir* 12 (1996) 1149.

- [53] R. Zana, *Adv. Colloid Interface Sci.* 97 (2002) 205 and references there in.
- [54] (a) M. Ao, P. Huang, G. Xu, X. Yang and Y. Wang, *Colloid Polym. Sci.* 287 (2009) 395; (b) J. Hoque, P. Kumar, V. K. Aswal and J. Haldar, *J. Phys. Chem. B* 116 (2012) 9718.
- [55] P. J. Tummino, A. Gafni, *Biophys. J.* 64 (1993) 1580.
- [56] E. Iglesias, L. Montenegro, *Phys. Chem. Chem. Phys.* 1 (1999) 4865.
- [57] K. Ludzik, H. Piekaeski, K. Kubalczyk, M. Wasiak, *Thermochimica Acta* 558 (2013) 29.
- [58] G. D. Noudeh, M. Housaindokht, B. S. F. Bazzaz, *J. App. Sci.* 7 (1994) 45.
- [59] B. Sarkar, S. Lam, P. Alexandridis, *Langmuir* 26 (2010) 10532.
- [60] I. Chakraborty, S. P. Moulik, *J. Phys. Chem. B* 111 (2007) 3658.
- [61] H. Rehage, H. J. Hoffmann, *Phys. Chem.* 92 (1988) 4712.
- [62] K-H. Kang, H-U. Kim, K-H, Lim, *Colloid Surf. A* 189 (2001) 113.
- [63] L. Grosmaire, M. Chorro, C. Chorro, S. Partyka, R. Zana, *J. Colloid Interface Sci.* 246 (2002) 175.
- [64] L. Grosmaire, M. Chorro, C. Chorro, S. Partyka, S. Lagerge, *Thermochimica Acta* 379 (2001) 255.
- [65] N. Hattori, A. Yoshino, H. Okabayashi, C. J. O'Connor, *J. Phys. Chem. B* 102 (1998) 8965
- [66] J. J. H. Nusselder, J. B. F. N. Engberts, *J. Colloid Interface Sci.* 148 (1992) 353.
- [67] Y. Han, Y. Wang, *Phys. Chem. Chem. Phys.* 13 (2011) 1939.